© 2014. Published by The Company of Biologists Ltd | Development (2014) 141, 3112-3122 doi:10.1242/dev.106336

RESEARCH ARTICLE

STEM CELLS AND REGENERATION

Hand2 elevates cardiomyocyte production during zebrafish heart development and regeneration

Yocheved L. Schindler[1,2], Kristina M. Garske[1], Jinhu Wang[3], Beth A. Firulli[4], Anthony B. Firulli[4], Kenneth D. Poss[3] and Deborah Yelon[1,2,*]

ABSTRACT

Embryonic heart formation requires the production of an appropriate number of cardiomyocytes; likewise, cardiac regeneration following injury relies upon the recovery of lost cardiomyocytes. The basic helix-loop-helix (bHLH) transcription factor Hand2 has been implicated in promoting cardiomyocyte formation. It is unclear, however, whether Hand2 plays an instructive or permissive role during this process. Here, we find that overexpression of *hand2* in the early zebrafish embryo is able to enhance cardiomyocyte production, resulting in an enlarged heart with a striking increase in the size of the outflow tract. Our evidence indicates that these increases are dependent on the interactions of Hand2 in multimeric complexes and are independent of direct DNA binding by Hand2. Proliferation assays reveal that *hand2* can impact cardiomyocyte production by promoting division of late-differentiating cardiac progenitors within the second heart field. Additionally, our data suggest that *hand2* can influence cardiomyocyte production by altering the patterning of the anterior lateral plate mesoderm, potentially favoring formation of the first heart field at the expense of hematopoietic and vascular lineages. The potency of *hand2* during embryonic cardiogenesis suggested that *hand2* could also impact cardiac regeneration in adult zebrafish; indeed, we find that overexpression of *hand2* can augment the regenerative proliferation of cardiomyocytes in response to injury. Together, our studies demonstrate that *hand2* can drive cardiomyocyte production in multiple contexts and through multiple mechanisms. These results contribute to our understanding of the potential origins of congenital heart disease and inform future strategies in regenerative medicine.

KEY WORDS: Hand2, Zebrafish, First heart field, Second heart field, Cardiac regeneration

INTRODUCTION

The assembly of the embryonic heart is a complex procedure involving the differentiation, migration and organization of the proper number of cardiomyocytes in order to form a functional contractile organ. Regulation of the genesis of cardiomyocytes requires the specification of heart fields with appropriate boundaries, as well as the controlled proliferation of the progenitor cells that emerge from these fields. An understanding of the genetic pathways that influence cardiomyocyte production may illuminate mutations that underlie congenital heart disease (CHD) (Fahed et al., 2013). Moreover, cardiomyocyte production, *in vitro* or *in vivo*, is a primary goal of cardiovascular regenerative medicine, and insight into genes that drive cardiomyocyte formation can enhance strategies for repairing hearts damaged by myocardial infarction (Laflamme and Murry, 2011; Choi and Poss, 2012; Xin et al., 2013). However, our understanding of the precise functions of factors that facilitate cardiomyocyte production remains incomplete.

The bHLH transcription factor Hand2 has been implicated as an important regulator of cardiomyocyte production. In mice, loss of *Hand2* function results in hypoplasia of the right ventricle and outflow tract (Srivastava et al., 1997), suggesting that *Hand2* promotes the development of cardiomyocytes derived from the second heart field (SHF). Furthermore, removal of *Hand2* function from the SHF via tissue-specific deletion of a conditional allele interferes with survival of this progenitor population (Tsuchihashi et al., 2011). The effects of loss of *Hand2* function are exacerbated when combined with either a conditional knockout or a hypomorphic allele of the related gene *Hand1*, suggesting functional redundancy between *Hand2* and *Hand1* that could mask earlier or broader roles of these factors in regulating cardiomyocyte production in mice (McFadden et al., 2005; Firulli et al., 2010).

In zebrafish, an early requirement for *hand2* during cardiomyocyte production has been clearly demonstrated. Zebrafish *hand2* mutants display a striking cardiac phenotype that features a dramatic deficit of cardiomyocytes (Yelon et al., 2000). This defect is evident from an early stage, as indicated by a substantial reduction in the number of cells that initiate expression of myocardial differentiation markers. Fate mapping has shown that *hand2* expression demarcates the heart-forming region within the anterior lateral plate mesoderm (ALPM), and, in *hand2* mutants, the progenitors residing in this region are ineffective at generating differentiated cardiomyocytes (Schoenebeck et al., 2007). Thus, *hand2* is important for facilitating cardiomyocyte production. However, it is not clear whether *hand2* regulates cardiomyocyte production by influencing cell fate decisions or by affecting proliferative capacity, nor is it known whether *hand2* plays an instructive or a permissive role in this setting.

The possibility that Hand2 instructively directs cardiomyocyte production has been highlighted by recent studies in which forced expression of *Hand2* was shown to increase the efficiency of reprogramming mammalian fibroblasts toward a myocardial fate (Song et al., 2012; Nam et al., 2013). Introduction of *Hand2*, *Gata4*, *Mef2c* and *Tbx5* into neonatal mouse fibroblasts increased the frequency of reprogramming approximately three- to fourfold over that observed with introduction of only *Gata4*, *Mef2c* and *Tbx5* (Song et al., 2012). Additionally, in human fibroblasts, *Hand2* has been shown to be essential for initiation of cardiac

[1]Division of Biological Sciences, University of California, San Diego, La Jolla, CA 92093, USA. [2]Developmental Genetics Program and Department of Cell Biology, Kimmel Center for Biology and Medicine, Skirball Institute of Biomolecular Medicine, New York University School of Medicine, New York, NY 10016, USA. [3]Department of Cell Biology, Howard Hughes Medical Institute, Duke University Medical Center, Durham, NC 27710, USA. [4]Riley Heart Research Center, Herman B. Wells Center for Pediatric Research, Departments of Pediatrics and Medical and Molecular Genetics, Indiana University School of Medicine, Indianapolis, IN 46202, USA.

*Author for correspondence (dyelon@ucsd.edu)

Received 21 November 2013; Accepted 17 June 2014

Development (2014) 141, 3112-3122 doi:10.1242/dev.106336

contractile gene expression programs during reprogramming, whereas other factors, such as *Gata4*, *Mef2c*, *Tbx5* and *Myocd*, play redundant roles in this regard (Nam et al., 2013). Thus, Hand2 can play a pivotal part in enhancing protocols for cardiac regeneration and repair; however, little is known about how forced expression of Hand2 mediates this role.

To gain new insight into the ability of Hand2 to drive cardiomyocyte production, we have examined the effects of *hand2* overexpression on the embryonic and adult zebrafish heart. We find that overexpression of *hand2* in the early embryo can increase cardiomyocyte numbers, with a particularly striking impact on the size of the cardiac outflow tract. Our data suggest that this cardiac enlargement results from increased progenitor proliferation within the SHF, as well as from increased cardiomyocyte specification within the first heart field (FHF). In addition, we find that overexpression of *hand2* in the adult heart enhances myocardial proliferation following injury. Together, our data suggest that *hand2* can play important and instructive roles in elevating cardiomyocyte production in multiple contexts: by promoting specification of FHF cardiomyocytes, by enhancing proliferation of SHF cardiac progenitors and by augmenting proliferation of regenerating cardiomyocytes. These results refine our understanding of the origins of CHD, particularly in the context of partial trisomy distal 4q, which involves duplication of *HAND2* (Tamura et al., 2013). Moreover, our findings highlight ways in which *hand2* overexpression could facilitate future approaches for cardiac regeneration and repair.

RESULTS

Overexpression of *hand2* increases cardiomyocyte production

To determine whether increased *hand2* function can enhance cardiomyocyte production, we injected zebrafish embryos with *hand2* mRNA. Although we have previously injected *hand2* mRNA into wild-type embryos (Yelon et al., 2000; Garavito-Aguilar et al., 2010), our prior studies did not closely examine its impact on heart size. Here, we found that injected embryos exhibited expanded expression of *cmlc2*, a marker of differentiated cardiomyocytes, within the ALPM at 18 somites (Fig. 1A,B). Measurements of the region of *cmlc2* expression revealed a significant increase in area within the *hand2*-overexpressing embryos (Fig. 1E). To examine whether increased *hand2* expression leads to enhanced heart size at later stages, we injected *hand2* mRNA into embryos carrying *Tg(-5.1myl7:nDsRed2)* (Mably et al., 2003), which facilitates quantification of fluorescent cardiomyocyte nuclei, and counted the number of cardiomyocytes present in the heart at 36 h post-fertilization (hpf). We found a significant increase in cardiomyocyte number in embryos overexpressing *hand2* (Fig. 1F). Together, these data suggest that increased expression of *hand2* can expand the heart-forming region within the ALPM, leading to a larger heart. However, *hand2* overexpression did not induce *cmlc2* expression outside the ALPM, indicating that cardiomyocyte production depends on the interaction of Hand2 with other ALPM factors.

The influence of Hand2 on cardiomyocyte production is dependent on protein-protein interactions and not on direct DNA binding

Previous studies have shown that Hand2 can function independently of direct DNA binding in some contexts (McFadden et al., 2002; Liu et al., 2009). Mice in which the *Hand2* gene was replaced with a DNA binding-deficient form of *Hand2* exhibited relatively normal hearts at E11.5 (Liu et al., 2009), in contrast to the severe ventricular hypoplasia seen in *Hand2* mutants by E10.5 (Srivastava et al., 1997). It is presumed that the DNA binding-deficient form of Hand2 can influence transcription through dimerization with other bHLH factors, as well as through interactions with larger protein complexes (Rychlik et al., 2003; Xu et al., 2003). To test whether the early role of *hand2* during cardiomyocyte production is dependent on DNA binding or dimerization, we evaluated whether previously characterized DNA binding-deficient and dimerization-deficient versions of Hand2 can expand *cmlc2* expression.

Replacement of three arginines (residues 109-111) in the basic domain of mouse Hand2 with acidic residues [glutamic acid, aspartic acid and glutamic acid (EDE)] has been shown to abolish DNA binding (McFadden et al., 2002; Liu et al., 2009). This region is highly conserved between mouse and zebrafish (supplementary material Fig. S1): 98% of the amino acids in the basic helix-loop-helix domain are identical, including these three arginine residues (100-102 in zebrafish). In addition, replacement of a phenylalanine (residue 119) with a proline in the first helix of mouse Hand2 has been shown to disrupt its dimerization (McFadden et al., 2002). This highly conserved amino acid is present in zebrafish Hand2 (F110; supplementary material Fig. S1). Extrapolating from prior work in

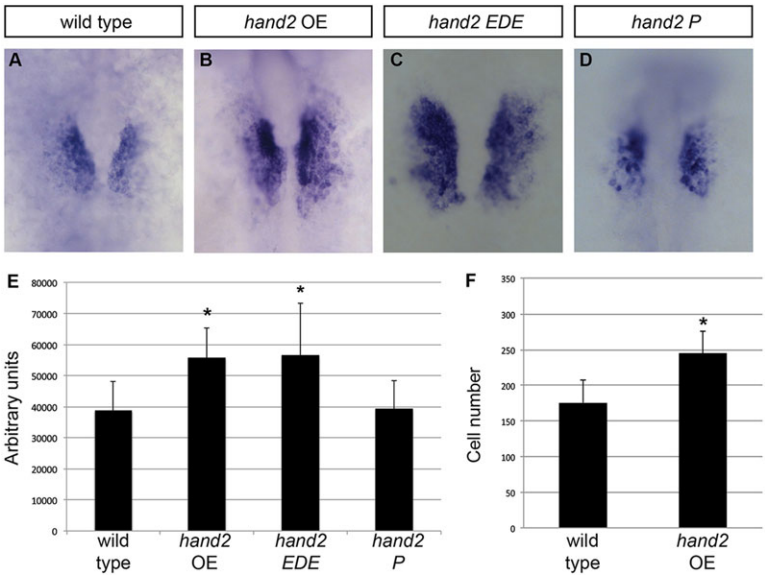

Fig. 1. *hand2* overexpression increases cardiomyocyte production. (A-D) *In situ* hybridization depicts *cmlc2* expression at 18 somites in (A) wild-type embryos, (B) *hand2*-overexpressing embryos (*hand2* OE), (C) embryos expressing a DNA binding-deficient form of *hand2* (*hand2 EDE*) and (D) embryos expressing a dimerization-deficient form of *hand2* (*hand2 P*); dorsal views, anterior upwards. Broader expression of *cmlc2* is found within the ALPM of embryos overexpressing *hand2* or *hand2 EDE*. (E) Average area of *cmlc2* expression, in arbitrary units, in wild-type embryos and in embryos overexpressing *hand2*, *hand2 EDE* or *hand2 P*. Error bars indicate s.d.; asterisks indicate significant differences from wild type. Overexpression of *hand2* or *hand2 EDE* increases area of *cmlc2* expression (n=13-25; *P<0.001), whereas overexpression of *hand2 P* does not (n=11; P=0.87). (F) Bar graph compares average number of cardiomyocytes at 36 hpf in wild-type embryos and in embryos overexpressing *hand2*. Error bars indicate s.d.; asterisk indicates a significant increase compared with wild type (n=17-19; *P<0.001).

Development (2014) 141, 3112-3122 doi:10.1242/dev.106336

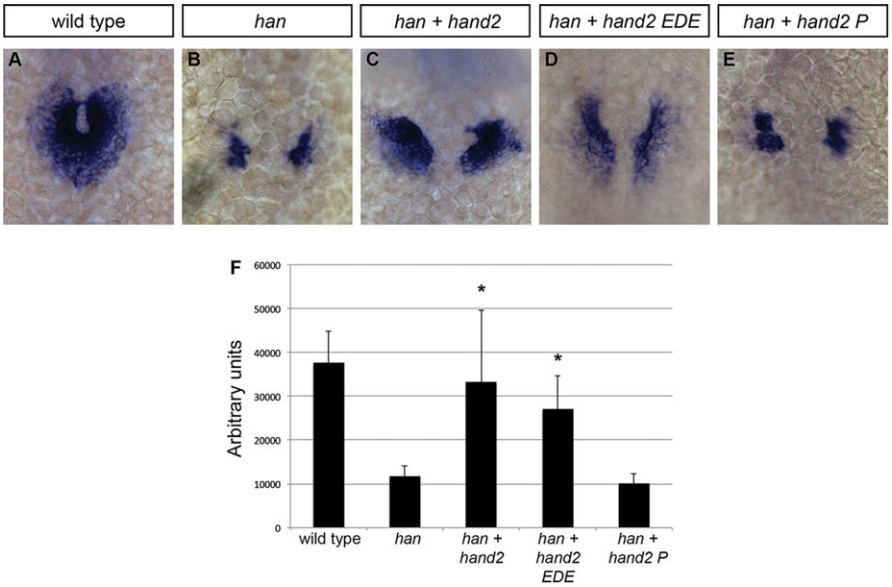

Fig. 2. Influence of Hand2 on cardiomyocyte production is dependent on dimerization and not on direct DNA binding. (A-E) *In situ* hybridization depicts *cmlc2* expression at 21 somites in (A) wild-type embryos, (B) *han*^{s6} mutant embryos, (C) *han*^{s6} mutant embryos injected with *hand2* mRNA, (D) *han*^{s6} mutant embryos injected with *hand2 EDE* mRNA and (E) *han*^{s6} mutant embryos injected with *hand2 P* mRNA; dorsal views, anterior upwards. The *han*^{s6} mutation is a null allele of *hand2* resulting from a deletion that removes the entire *hand2* gene (Yelon et al., 2000). At this stage, wild-type cardiomyocytes have formed a ring (A), whereas few cardiomyocytes have formed in the *han*^{s6} mutants (B). Cardiomyocyte formation is substantially rescued with the injection of *hand2* (C) or *hand2 EDE* (D) mRNA, but not of *hand2 P* mRNA (E). (F) Average area of *cmlc2* expression, as in Fig. 1E. Asterisks indicate significant differences between the phenotype of *han*^{s6} mutant embryos and the phenotypes of *han*^{s6} mutant embryos overexpressing versions of *hand2*. Overexpression of *hand2* or *hand2 EDE* partially rescues the area of *cmlc2* expression in *han*^{s6} mutants (n=14; *P<0.001), whereas *hand2 P* does not (n=14; P=0.085).

mouse, we constructed corresponding variants of zebrafish *hand2* and injected mRNA encoding each variant into wild-type embryos. Overexpression of the DNA binding-deficient form of *hand2* (*hand2 EDE*) expanded the area of *cmlc2* expression in a manner similar to the overexpression of wild-type *hand2* (Fig. 1A-C,E). However, overexpression of the dimerization-deficient version of *hand2* (*hand2 P*) did not expand the *cmlc2* expression domain (Fig. 1A,D,E). Furthermore, injection of *hand2 EDE* mRNA substantially rescued *cmlc2* expression in embryos homozygous for a null allele of *hand2* (*han*^{s6}) (Yelon et al., 2000), reminiscent of the effects of injecting wild-type *hand2* into *han*^{s6} mutants (Fig. 2A-D,F). By contrast, injection of *hand2 P* mRNA did not alter *cmlc2* expression in *han*^{s6} mutants (Fig. 2B,E,F). These results suggest that Hand2 dimerization, but not its direct binding to DNA, is necessary for its influence on cardiomyocyte production.

Induction of *hand2* overexpression after gastrulation expands cardiomyocyte production

In some embryos injected with *hand2* mRNA, we observed morphological defects that could result from abnormal gastrulation, such as shortened body axis or abnormal body curvature. To bypass effects on gastrulation, we established an inducible system for *hand2* overexpression. We constructed a series of transgenes in which *hand2* is transcribed under the control of the *hsp70* heat shock promoter (Halloran et al., 2000). In these transgenes, we connected Hand2 to mCherry using the viral 2A peptide sequence that allows separate stoichiometric translation of both proteins in order to facilitate monitoring of transgene expression after heat shock (Provost et al., 2007; Covassin et al., 2009).

In embryos carrying *Tg(hsp70:FLAG-hand2-2A-mCherry)* [hereafter referred to as *Tg(hsp70:hand2)*], induction of *hand2* overexpression after gastrulation was sufficient to cause a cardiac phenotype similar to that caused by mRNA injection at the one-cell stage. After heat shock at 10 hpf (tail bud stage), transgenic embryos overexpressing *hand2* exhibited a significant expansion in *cmlc2* expression at 18 somites (Fig. 3A,B,E), as well as a significant increase in cardiomyocyte number at 36 hpf (Fig. 3F), compared with their heat-shocked nontransgenic siblings. Heat-shocked transgenic embryos also displayed a pronounced pericardial edema (supplementary material Fig. S2A,B) and an enlarged heart with a noticeably extended outflow tract (Fig. 3G,I). In contrast to the consequences of *hand2* induction at 10 hpf, induction of *hand2* overexpression at 24 hpf resulted in an embryo without evident pericardial edema (supplementary material Fig. S2C) or outflow tract enlargement (Fig. 3H). These data suggest that *hand2* has a potent influence on cardiomyocyte production between 10 and 24 hpf, after gastrulation and before the initial assembly of the heart tube.

The cardiac expansion induced by *hand2* overexpression requires phosphorylation-independent dimerization of Hand2

The consequences of injection of the *hand2 EDE* and *hand2 P* mRNAs suggest that the role of Hand2 during cardiomyocyte production requires its dimerization but not its direct binding to DNA (Fig. 2). Phosphorylation of conserved threonine and serine residues within the first helix of Hand factors has previously been shown to be important for their choice of dimerization partners (Firulli et al., 2003, 2005). For example, changes in phosphorylation of T107 and S109 of mouse Hand1 influence the affinity for formation of Hand1-Hand1 homodimers relative to the formation of Hand1 heterodimers with E proteins (Firulli et al., 2003). To determine whether the dimerization interactions that influence cardiomyocyte production require Hand2 phosphorylation, we constructed the transgene *Tg(hsp70:FLAG-hand2*^{AA}*-2A-mCherry)* [referred to as *Tg(hsp70:hand2*^{AA}*)*]. The zebrafish Hand2 variant

Development (2014) 141, 3112-3122 doi:10.1242/dev.106336

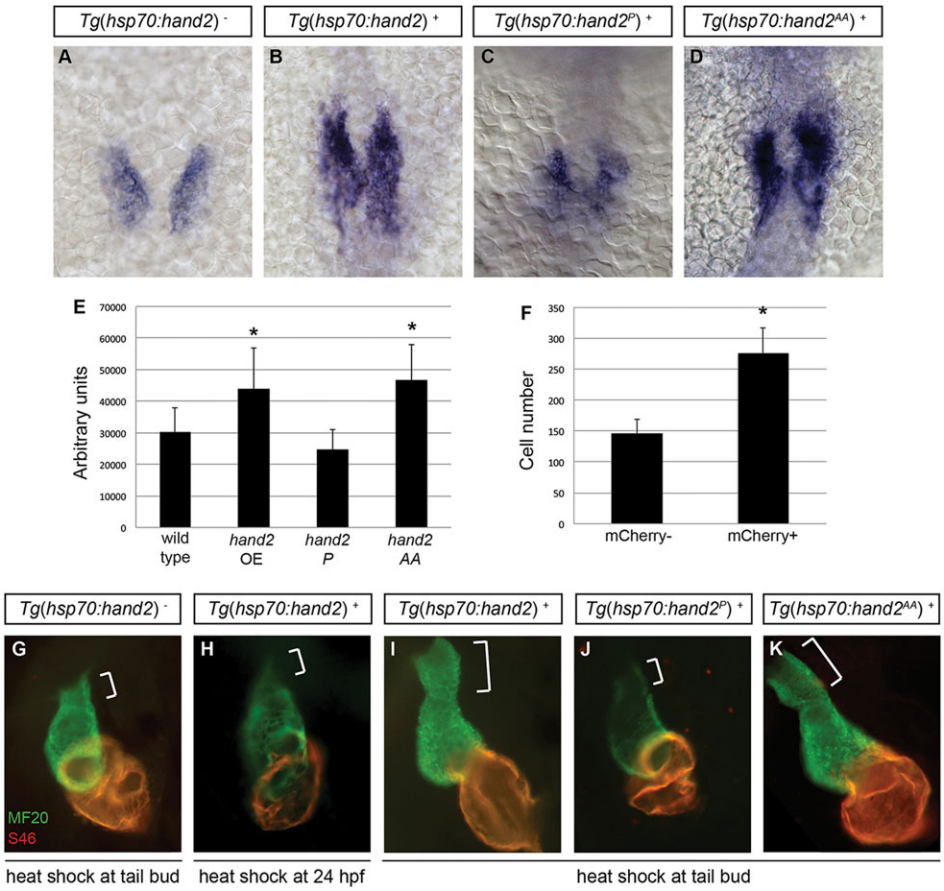

Fig. 3. Cardiac expansion induced by *hand2* overexpression requires phosphorylation-independent dimerization of Hand2. (A-D) *In situ* hybridization depicts *cmlc2* expression at 18 somites in (A) nontransgenic embryos, (B) *Tg(hsp70:hand2)* embryos, (C) *Tg(hsp70:hand2^{P})* embryos and (D) *Tg(hsp70:hand2^{AA})* embryos, heat-shocked at 10 hpf; dorsal views, anterior upwards. (E) Average area of *cmlc2* expression, as in Fig. 1E, in nontransgenic and transgenic embryos, following heat shock at 10 hpf. Asterisks indicate significant differences from nontransgenic embryos. Overexpression of *hand2* or *hand2 AA* increases the area of *cmlc2* expression (n=15-32; *P<0.001), whereas *hand2 P* does not (n=13; P=0.05). (F) Average number of cardiomyocytes at 36 hpf, as in Fig. 1F, in nontransgenic embryos and in *Tg(hsp70:hand2)* embryos, following heat shock at 10 hpf. Asterisk indicates a significant difference from nontransgenic embryos (n=16-20; *P<0.001). (G-K) Immunofluorescence at 36 hpf for MF20 (green, visible in the ventricle) and S46 (red, visible in the atrium) shows cardiac morphology. Frontal views; brackets mark the outflow tract. Hearts of *Tg(hsp70:hand2)* embryos heat-shocked at 24 hpf (H) resemble nontransgenic hearts heat-shocked at 10 hpf (G). *Tg(hsp70:hand2)* embryos heat-shocked at 10 hpf (I) show an overall increase in cardiac size and an enlarged outflow tract. Similar morphology is seen after heat shock at 10 hpf in *Tg(hsp70:hand2^{AA})* embryos (K), but not in *Tg(hsp70:hand2^{P})* embryos (J).

expressed by this transgene features substitution of the residues T103 and S105 with alanines (supplementary material Fig. S1), thereby preventing their phosphorylation; extrapolating from prior studies of Hand1 and Twist1, these changes may promote affinity for homodimerization rather than heterodimerization with E proteins (Firulli et al., 2003, 2005).

We compared the effects of inducing expression of *hand2*, *hand2^{AA}* and *hand2^{P}*, using inducible transgenes to overexpress each variant (supplementary material Fig. S3). Induction of expression of the phosphorylation-deficient version of *hand2* at 10 hpf resulted in expansion of *cmlc2* expression at 18 somites, similar to the effects of inducing wild-type *hand2* expression (Fig. 3A,B,D,E). Likewise, overexpression of the phosphorylation-deficient version of *hand2* caused formation of an enlarged heart and an elongated outflow tract by 36 hpf, as is the case for overexpression of wild-type *hand2* (Fig. 3G,I,K). By contrast, induction of expression of the dimerization-deficient version of *hand2* did not expand the area of *cmlc2* expression (Fig. 3C,E) and did not yield a larger heart or outflow tract (Fig. 3J). These data suggest that an unphosphorylated form of Hand2 mediates its dimerization and role in the context of cardiac expansion.

Increased proliferation in late-differentiating cells contributes to cardiac expansion in embryos overexpressing *hand2*

The enlarged hearts in embryos overexpressing *hand2* led us to investigate the cellular mechanism through which *hand2* influences cardiomyocyte expansion. As overexpression of *Hand1* has been shown to enhance proliferation within the outflow tract in mice (Risebro et al., 2006), we were especially interested in determining the origins of the elongated outflow tract in *hand2*-overexpressing embryos. First, we examined the expression of *mef2cb* at 36 hpf; at this stage, *mef2cb* marks a population of SHF-derived cells that contributes to the outflow tract (Lazic and Scott, 2011; Hinits et al., 2012). We found excess *mef2cb* expression at the arterial pole of the heart in *hand2*-overexpressing embryos (Fig. 4A-D), suggesting that the observed outflow tract expansion is the product of excess SHF-derived cells, rather than simply a morphological anomaly. In addition, *mef2cb* expression in embryos overexpressing the phosphorylation-deficient and dimerization-deficient versions of *hand2* correlated with the observed outflow tract morphologies: embryos overexpressing *hand2 AA* exhibited an excess of *mef2cb*-expressing cells (Fig. 4G,H), whereas embryos overexpressing *hand2 P* did not (Fig. 4E,F). In contrast to their expanded *mef2cb* expression at the arterial pole, *hand2*-overexpressing embryos exhibited a normal pattern of *islet1* expression at the venous pole (supplementary material Fig. S4), suggesting that *hand2* has a more potent influence on outflow tract formation than on inflow tract formation.

Next, we employed an EdU incorporation assay to investigate whether the expansion of the outflow tract or the general increase in cardiomyocyte number could be the result of increased proliferation in *hand2*-overexpressing embryos. Following heat shock at 10 hpf, we pulsed embryos with EdU for 30 min when they reached 17 hpf, thereby labeling proliferating cells during that interval (Fig. 5G). We then compared the numbers of EdU-positive and EdU-negative cardiomyocytes at 36 hpf in *Tg(hsp70:hand2)* embryos and their nontransgenic siblings (Fig. 5A-F). Strikingly, we found a significantly higher proliferation index in the *hand2*-overexpressing cardiomyocytes (Fig. 5H), indicating that increased proliferation

Development (2014) 141, 3112-3122 doi:10.1242/dev.106336

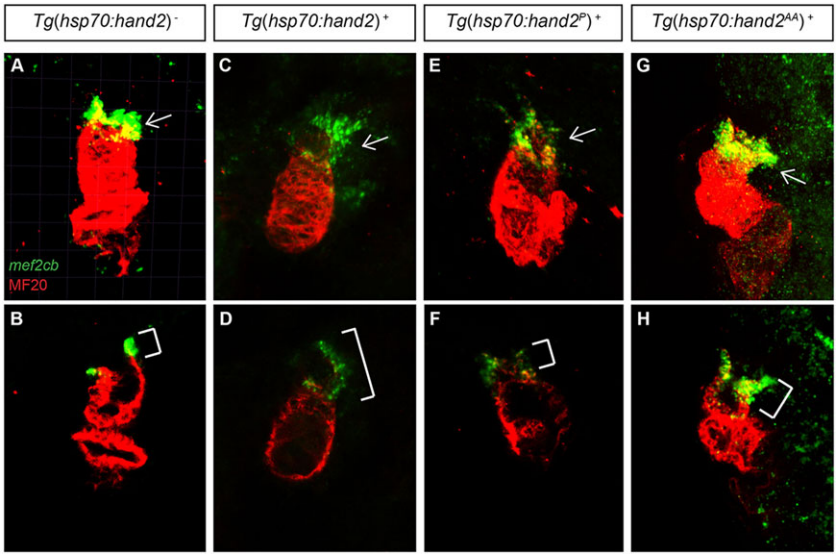

Fig. 4. Overexpression of *hand2* causes outflow tract expansion. (A-H) MF20 antibody staining (red) and *mef2cb in situ* hybridization (green) at 36 hpf in (A,B) nontransgenic, (C,D) *Tg(hsp70:hand2)*, (E,F) *Tg(hsp70:hand2^{P})* and (G,H) *Tg(hsp70:hand2^{AA})* embryos, all of which were heat-shocked at 10 hpf. Frontal views; (A,C,E,G) partial reconstructions of confocal *z*-stacks with arrows indicating outflow tract; (B,D,F,H) single slices with brackets marking outflow tract. Embryos overexpressing *hand2* (C,D) or *hand2 AA* (G,H) exhibit expanded populations of *mef2cb*-expressing cells, whereas embryos overexpressing *hand2 P* (E,F) do not.

contributes to the enhanced cardiomyocyte production in these embryos. By contrast, in a parallel set of experiments in which we pulsed embryos with EdU at 23 hpf (supplementary material Fig. S5A-G), we did not detect an increased proliferation index in *hand2*-overexpressing cardiomyocytes (supplementary material Fig. S5H), suggesting that *hand2* overexpression influences proliferation prior to 23 hpf.

Based on this series of results, we hypothesized that increased proliferation in *hand2*-overexpressing embryos occurs between 17 hpf and the time of initial heart tube assembly. To test this, we pulsed embryos with EdU at 17 hpf and analyzed the distribution of EdU-positive cells at 26 hpf in *hand2*-overexpressing and nontransgenic embryos (Fig. 6A-E). In addition to scoring EdU-positive cardiomyocytes, we used *Tg(nkx2.5:ZsYellow)* to facilitate scoring of EdU labeling in SHF-derived progenitor cells that reside near the arterial pole of the early heart tube and ultimately contribute to the outflow tract (Zhou et al., 2011); these progenitor cells express *Tg(nkx2.5:ZsYellow)* but do not yet express high levels of other myocardial differentiation markers. In these experiments, we found that *hand2* overexpression caused a significant increase in the proliferation index of the SHF-derived cardiac progenitor cells near the arterial pole (Fig. 6F). However, *hand2* overexpression did not enhance the proliferation index of the first heart field-derived (FHF-derived) cardiomyocytes that form the initial heart tube (Fig. 6F); we obtained similar results when assessing the cardiomyocyte proliferation index in embryos pulsed with EdU at 17 hpf and fixed at 23 hpf, and in embryos pulsed with EdU at 14 hpf and fixed at 26 hpf (supplementary material Fig. S6). Altogether, our data demonstrate that overexpression of *hand2* has a potent and early impact on the proliferation of the SHF-derived, late-differentiating progenitor cells that will create the outflow tract.

Overexpression of *hand2* alters ALPM patterning

Although our results suggest that enhanced proliferation of SHF-derived progenitors contributes to the enlarged outflow tract seen when *hand2* is overexpressed, increased proliferation within the SHF may not account for all of the enhanced cardiomyocyte production in *hand2*-overexpressing embryos. Notably, the increased area of *cmlc2* expression observed at 18 somites (Fig. 3A,B,E) seems to reflect increased production of cardiomyocytes by the FHF, as only early-differentiating, FHF-derived cells are thought to express *cmlc2* at this stage (de Pater et al., 2009). Additionally, we have found increased numbers of differentiated cardiomyocytes in *hand2*-overexpressing embryos at 23 hpf (nontransgenic embryos, 127±25 cardiomyocytes; *hand2*-overexpressing embryos, 164±39 cardiomyocytes; n=9 or 10, P<0.05) and at 26 hpf (nontransgenic embryos, 154±25 cardiomyocytes; *hand2*-overexpressing embryos, 224±47 cardiomyocytes; n=10 or 11, P<0.001). As is the case at 18 somites, it is thought that cardiomyocytes have not yet been added from the SHF at 23 or 26 hpf (de Pater et al., 2009; Lazic and Scott, 2011). Furthermore, we did not detect an increased proliferation index in the cardiomyocyte population at 23 or 26 hpf (Fig. 6F; supplementary material Fig. S6F). Together, these data suggest that the early expansion of cardiomyocytes in *hand2*-overexpressing embryos reflects an influence of *hand2* on the early-differentiating FHF, and that this effect is more likely to be the result of altered specification than of altered proliferation.

To evaluate whether overexpression of *hand2* alters the patterning of the ALPM, we examined markers of lineages that are neighbors of the heart fields at early stages. *scl* and *etsrp* are expressed in progenitors of the blood and vessel lineages that are rostral to the heart-forming region that expresses *hand2* (Schoenebeck et al., 2007). When blood and vessel lineage specification are inhibited by loss of *scl* and *etsrp* function, *hand2* expression expands into the rostral ALPM and an increased number of cardiomyocytes form (Schoenebeck et al., 2007; Palencia-Desai et al., 2011). These findings suggest that *scl* and *etsrp* act to limit the extent of myocardial specification in the ALPM. Conversely, we found that overexpression of *hand2* limited the expression of anterior hematopoietic and endothelial markers at 12 somites, including *scl*, *etsrp* and *pu.1* (Fig. 7A-F); even so, these gene expression defects did not seem to cause major anomalies in vascular patterning or in endocardial development (supplementary material Fig. S7). At the same time, *hand2*-overexpressing embryos exhibited expanded expression of *mef2cb* (Fig. 7G,H), which is found in myocardial progenitor cells at this stage (Hinits et al., 2012). However, not all myocardial progenitor markers are similarly expanded, as we found that *hand2*-overexpressing embryos exhibit normal expression of *nkx2.5* at 12 somites (Fig. 7I,J). This result suggests that *hand2* functions downstream of *nkx2.5*, which is consistent with the normal *nkx2.5* expression pattern observed in *hand2* mutant embryos (Yelon et al., 2000; Schoenebeck et al., 2007). Finally, *gata4* expression also appeared

Development (2014) 141, 3112-3122 doi:10.1242/dev.106336

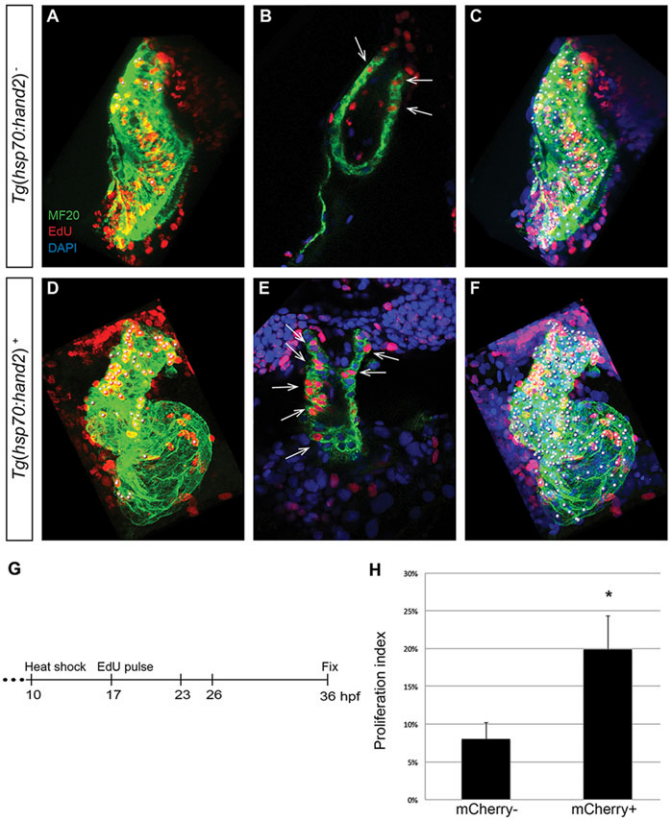

Fig. 5. Increased proliferation contributes to cardiac expansion in *hand2*-overexpressing embryos. (A-F) EdU incorporation in hearts of (A-C) nontransgenic and (D-F) *Tg(hsp70:hand2)* embryos at 36 hpf, following heat shock at 10 hpf and EdU pulse at 17 hpf. Partial reconstructions of confocal *z*-stacks with ventricle upwards (A,C,D,F) and representative single slices (B,E). (A,D) White dots indicate EdU-positive (red) cells that are also MF20-positive (green) differentiated cardiomyocytes. (B,E) Arrows indicate EdU-positive cells that are also MF20 positive; DAPI (blue) marks all nuclei. (C,F) White dots indicate all myocardial nuclei. Qualitative assessment suggests increased numbers of EdU-positive cardiomyocytes in *hand2*-overexpressing hearts (D,E), particularly in the distal region of the ventricle and the outflow tract. (G) Timeline of experimental design. (H) Proliferation indices in nontransgenic (mCherry-negative) and *Tg(hsp70:hand2)* (mCherry-positive) embryos; error bars indicate s.d. Proliferation index was calculated by dividing the number of EdU-positive cardiomyocytes by the total number of cardiomyocytes. A significant increase in proliferation index was evident in *hand2*-overexpressing embryos (n=8 or 9; *P<0.001).

similar in nontransgenic and *hand2*-overexpressing embryos (Fig. 7K,L), indicating that increased *hand2* expression does not alter the overall dimensions of the ALPM. Thus, in addition to a later capacity to promote proliferation within the SHF, *hand2* overexpression can influence early patterning processes within the ALPM, possibly by promoting myocardial specification while limiting hematopoietic and endothelial specification.

Overexpression of *hand2* augments cardiomyocyte proliferation during cardiac regeneration

Mechanisms of embryonic heart development have served as necessary guides for understanding cardiac regeneration. The potent effects of *hand2* in the early embryo raise the possibility that its expression could influence the efficacy of regeneration in the injured adult heart. In the zebrafish, cardiac injuries are repaired through a process in which spared mature cardiomyocytes reduce indicators of differentiation and proliferate to regenerate lost muscle, involving induction and function of *gata4* in source cardiomyocytes (Jopling et al., 2010; Kikuchi et al., 2010; Gupta et al., 2013). In previous studies, we also observed increased expression of *nkx2.5*, *tbx5* and *tbx20* in the injury site following resection of the adult zebrafish ventricle (Lepilina et al., 2006), although the induction of these genes was not detectable by others (Raya et al., 2003; Jopling et al., 2010). We additionally found activation of *hand2* and *gata5* regulatory sequences in endocardial cells after resection injury (Kikuchi et al., 2011a). To assess gene expression after a more severe injury, we employed transgene-driven cardiomyocyte ablation in Z-CAT transgenic fish, in which the combination of *Tg(cmlc2:CreER)* and *Tg(β-actin2:loxp-mCherry-STOP-loxp-DTA)* transgenes permits 4-HT-inducible expression of diphtheria toxin in cardiomyocytes (Wang et al., 2011). Enhanced expression of *hand2*, as well as *nkx2.5*, *tbx5* and *tbx20*, was evident in spared cardiomyocytes throughout the injured Z-CAT ventricle (Fig. 8A-H). Additionally, fluorescence in *Tg(hand2:EGFP)* myocardium and endocardium was boosted during regeneration (Fig. 8I-K), indicating that cardiac injury can activate *hand2* regulatory sequences in multiple cell types.

To test whether induced *hand2* expression in adult cardiomyocytes affects their regenerative capacity, we first examined cardiomyocyte proliferation in injured Z-CAT animals heterozygous for the han^{s6} mutation (Yelon et al., 2000). Heterozygosity for han^{s6} did not alter levels of ablation-induced cardiomyocyte proliferation, although we also did not detect reduced levels of *hand2* mRNA in injured heterozygous hearts (data not shown). To artificially increase *hand2* expression in cardiomyocytes after injury, we generated a new transgene that permits 4-HT-inducible *hand2* expression, *Tg(β-actin2:loxp-mCherry-STOP-loxp-hand2)* [hereafter referred to as *Tg(β-actin2:RSH)*]. In fish carrying *Tg(β-actin2:RSH)* in combination with *Tg(cmlc2:CreER)*, a single 4-HT injection sharply increased myocardial *hand2* expression but had no effect on cardiomyocyte proliferation in the absence of injury (data not shown). In Z-CAT animals carrying *Tg(β-actin2:RSH)*, we experimentally elevated *hand2* levels in spared cardiomyocytes in concert with inducing ablation injury (Fig. 9A). Under these conditions, we observed a 34% increase in cardiomyocyte proliferation in Z-CAT; *Tg(β-actin2:RSH)* animals at 7 days post-injection (dpi), compared with that seen in Z-CAT animals at the same timepoint (Fig. 9B). To confirm effects of *hand2* on regenerative proliferation, we induced *hand2* overexpression in *Tg(cmlc2:CreER); Tg(β-actin2:RSH)* animals by injecting 4-HT 5 days before performing ventricular resection. In these experiments, we observed a 102% increase in cardiomyocyte proliferation at the resection plane, compared with the proliferation observed in vehicle-injected *Tg(cmlc2:CreER); Tg(β-actin2:RSH)* animals (Fig. 9C-E). In total, our results indicate that elevation of *hand2* expression helps boost cardiomyocyte production during regeneration, mirroring its effect in the embryo.

DISCUSSION

Taken together, our studies demonstrate three distinct mechanisms through which *hand2* overexpression can promote enhanced cardiomyocyte production. First, overexpression of *hand2* results in expansion of cardiomyocyte production within the early differentiating FHF, potentially by promoting myocardial specification at the expense of neighboring blood and vessel lineages. Second, *hand2* overexpression causes excess proliferation of cardiac progenitor cells within the late-differentiating SHF, leading to the formation of an abnormally elongated outflow tract. Third, induced myocardial expression of *hand2* enhances regenerative proliferation of cardiomyocytes in response to injury.

Development (2014) 141, 3112-3122 doi:10.1242/dev.106336

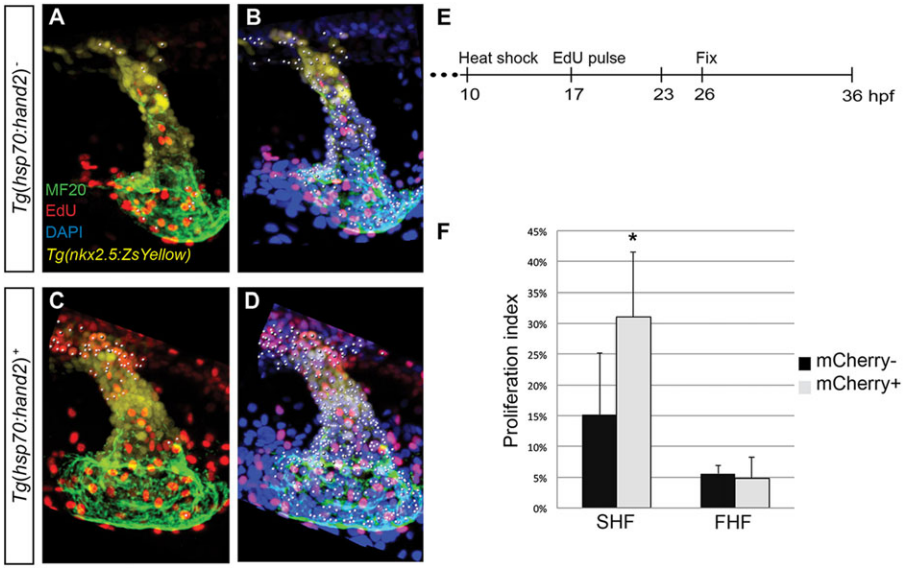

Fig. 6. Overexpression of *hand2* increases proliferation of SHF-derived progenitor cells. (A-D) EdU incorporation in (A,B) nontransgenic and (C,D) *Tg(hsp70:hand2)* embryos at 26 hpf, following heat shock at 10 hpf and EdU pulse at 17 hpf; partial reconstructions of confocal *z*-stacks with ventricle upwards. (A,C) White dots indicate EdU-positive (red) cells that are MF20 positive (green) and/or expressing *Tg(nkx2.5:ZsYellow)* (yellow). (B,D) White dots indicate all nuclei (DAPI, blue) of cells that are MF20 positive and/or expressing *Tg(nkx2.5:ZsYellow)*. (E) Timeline of experimental design. (F) Proliferation indices, as in Fig. 5H, for two populations of cells: SHF-derived cells, defined as *Tg(nkx2.5:ZsYellow)*-expressing cells with very low or no MF20 staining; and FHF-derived cells, defined as cells with clearly detectable MF20 staining. Proliferation index was calculated for each population independently by dividing the number of EdU-positive cells by the total number of cells in the population. A significant increase in proliferation index was evident in the SHF-derived cells in *hand2*-overexpressing embryos (n=10 or 11; *P=0.003), but not in the FHF-derived cells (n=10 or 11; P=0.528).

Our previous studies have shown that loss of *hand2* function dramatically reduces the cardiomyocyte population, emphasizing the necessity of *hand2* for efficient cardiomyocyte production (Yelon et al., 2000; Schoenebeck et al., 2007). Integrating our current and past work, we conclude that *hand2* plays important and instructive roles in promoting cardiomyocyte production via influences on both specification and proliferation.

Our data indicate that overexpression of *hand2* is sufficient to induce ectopic cardiomyocyte formation in a region proximal to the typical FHF, but we do not find ectopic cardiomyocytes elsewhere within *hand2*-overexpressing embryos. Additionally, while *hand2* overexpression is capable of hindering the expression of blood and vessel markers, *hand2*-null embryos do not exhibit expanded expression of blood and vessel genes (Schoenebeck et al., 2007). These findings suggest that other factors partner with Hand2 to promote myocardial specification in the FHF and that expression of these factors is restricted to a particular region of the ALPM. The significance of the partnerships between Hand2 and other factors is reinforced by our data demonstrating that the effects of *hand2* overexpression on cardiomyocyte production appear to be independent of direct binding of DNA by Hand2 and dependent on Hand2 dimerization. It will be valuable for future studies to investigate which Hand2 dimerization partners are relevant to its influences on ALPM patterning.

In addition to an instructive role for *hand2* during specification of the FHF, our data suggest a previously unappreciated role for *hand2* in promoting progenitor proliferation within the SHF. Hand factors have been shown to have roles in both promoting and inhibiting proliferation

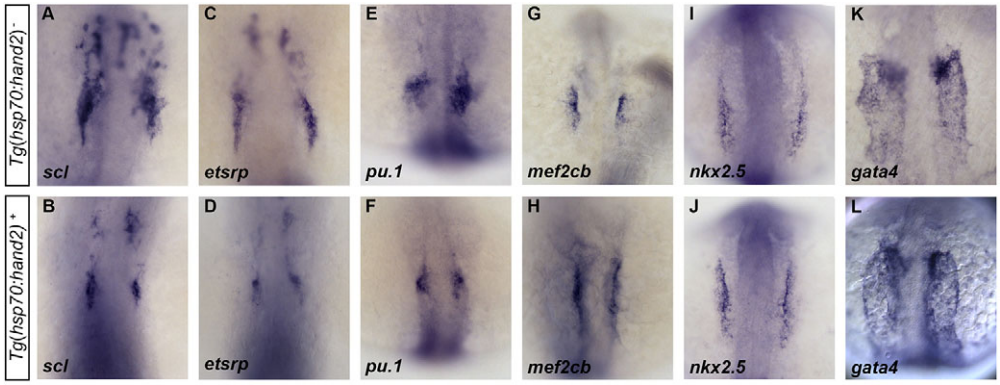

Fig. 7. *hand2* overexpression limits expression of blood and vessel genes within the ALPM. (A-L) *In situ* hybridization depicts expression of (A,B) *scl*, (C,D) *etsrp*, (E,F) *pu.1*, (G,H) *mef2cb*, (I,J) *nkx2.5* and (K,L) *gata4* in (A,C,E,G,I,K) nontransgenic embryos and (B,D,F,H,J,L) *Tg(hsp70:hand2)* embryos following heat shock at 10 hpf. Dorsal views, anterior upwards, at (A-J) 12 somites and (K,L) 10 somites. Overexpression of *hand2* results in (A-F) decreased distribution of *scl*, *etsrp* and *pu.1* expression, as well as (G,H) increased expression of *mef2cb*. By contrast, expression of (I,J) *nkx2.5* and (K,L) *gata4* appear relatively normal in *hand2*-overexpressing embryos at these stages.

Development (2014) 141, 3112-3122 doi:10.1242/dev.106336

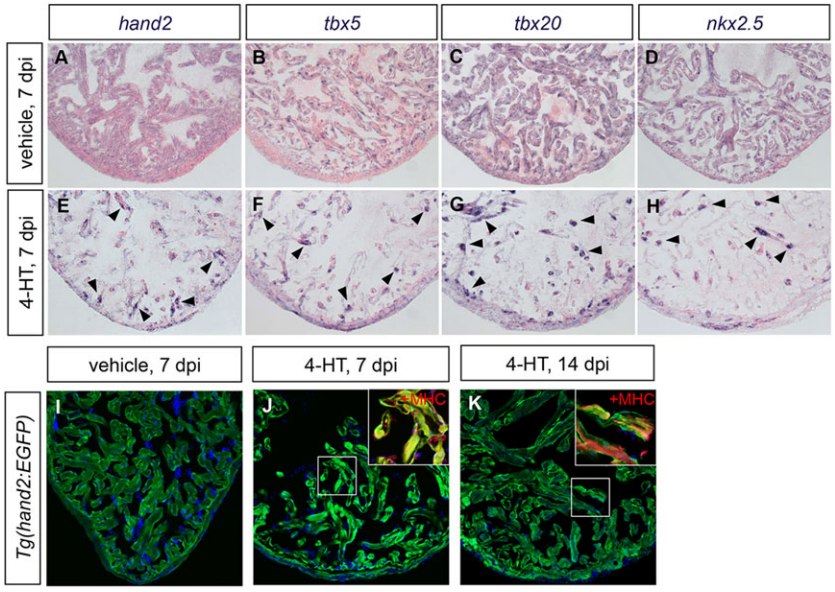

Fig. 8. Cardiac injury induces *hand2* expression. (A-H) *In situ* hybridization depicts expression of (A,E) *hand2*, (B,F) *tbx5*, (C,G) *tbx20* and (D,H) *nkx2.5* in ventricles of adult Z-CAT fish 7 days post-injection (dpi) of vehicle (A-D) or 4-HT (E-H). Expression of each gene is enhanced in spared myocardium following injury (E-H, arrowheads). (I-K) Expression of *Tg(hand2:EGFP)* (green) highlights the activation of *hand2* regulatory sequences following injury. Images are single confocal slices of ventricular tissue at 7 dpi (I,J) and 14 dpi (K); insets demonstrate myosin heavy chain (MHC; red) localization in *hand2*-expressing cells.

(Risebro et al., 2006; Li et al., 2011), but this particular role of *hand2* in the SHF has not been demonstrated by prior studies. The impact of *hand2* on SHF progenitor proliferation contrasts with previous work that found a role for *Hand2* in promoting survival of SHF progenitor cells (Tsuchihashi et al., 2011); although proliferation defects were not documented in these studies of conditional *Hand2* knockout mice, it is possible that deficient SHF proliferation preceded the observed death of SHF cells in these embryos. Additionally, it is interesting to compare the effects of *hand2* overexpression on the zebrafish SHF with the phenotype of mouse mutants in which *Hand1*-expressing cells were engineered to overexpress *Hand1* (Risebro et al., 2006). In these mice, increased proliferation was seen in the distal outflow tract, but no expansion of SHF progenitor markers was observed, suggesting that *Hand1* overexpression did not increase proliferation within the SHF itself but instead within the cardiomyocytes present or arriving at the outflow tract (Risebro et al., 2006). These effects of *Hand1* overexpression on outflow tract proliferation seem distinct from our observed effects of *hand2* overexpression on the SHF progenitor

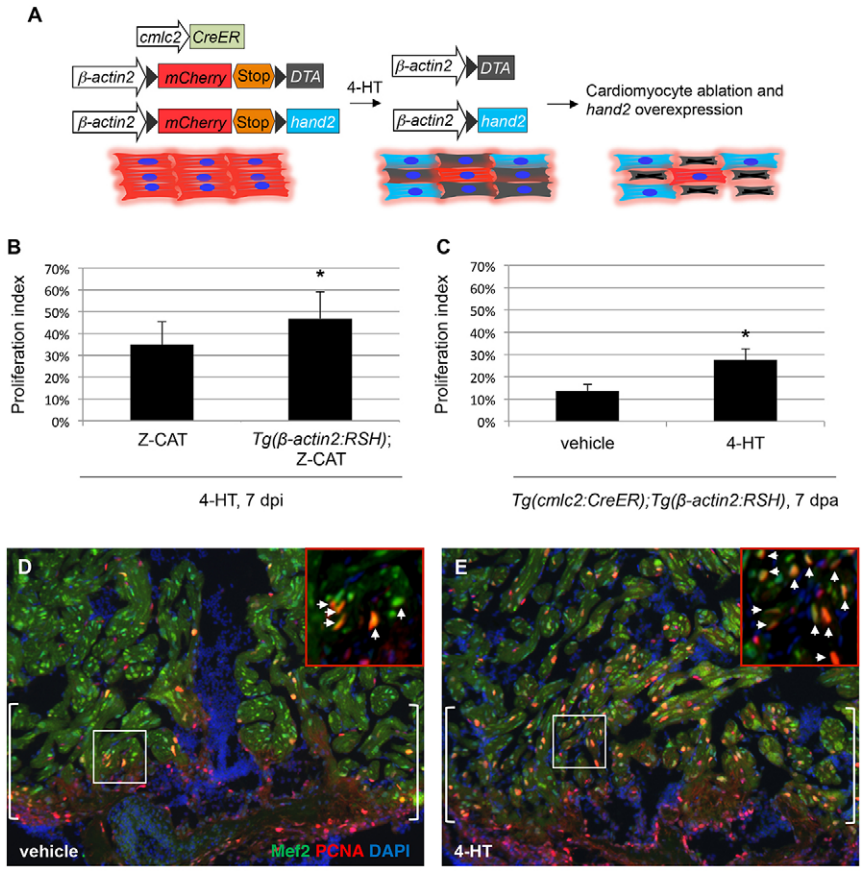

Fig. 9. Overexpression of *hand2* boosts cardiomyocyte proliferation in response to injury. (A) Schematic representation of transgenes used for cardiomyocyte ablation and myocardium-specific *hand2* overexpression in Z-CAT fish. (B) Proliferation indices for ventricular cardiomyocytes; error bars indicate s.e.m. Proliferation was assessed 7 days after 4-HT injection in Z-CAT fish with or without induced cardiomyocyte-specific *hand2* overexpression. *hand2*-overexpressing fish exhibited significantly increased proliferation following ablation injury (n=9 or 10; *P<0.05). (C) Proliferation indices in injured *cmlc2:CreER*; *β-act2:RSH* fish; error bars indicate s.e.m. Proliferation was assessed at the resection plane 7 days post-amputation (dpa) in animals that were injected with either vehicle or 4-HT 5 days before injury. *hand2*-overexpressing fish exhibited significantly increased proliferation following resection injury (n=4 or 5; *P<0.005). (D,E) Representative examples of cardiomyocyte proliferation at 7 dpa at the resection plane (brackets) in injured *cmlc2:CreER*; *β-act2:RSH* fish that were treated with vehicle (D) or 4-HT (E). Mef2 (green) marks cardiomyocytes and PCNA (red) marks proliferating cells; arrows in insets indicate double-positive cells.

Development (2014) 141, 3112-3122 doi:10.1242/dev.106336

population outside the heart tube; this difference may relate to the conditional regulation of *Hand1* expression in these mice, which do not overexpress *Hand1* within the SHF.

Finally, our data indicate that *hand2* overexpression can impact regenerative cardiomyocyte proliferation in the adult heart. These findings implicate the induction of *hand2* expression during regeneration as a key component of the regenerative mechanism. We speculate that the ability of Hand2 to increase reprogramming efficiency of fibroblasts toward a cardiac fate (Song et al., 2012; Nam et al., 2013) could be related to our observation that Hand2 can enhance cardiomyocyte proliferation; alternatively, the function of Hand2 during reprogramming could be a reflection of our observed influences of Hand2 on myocardial progenitor specification or proliferation. To distinguish between these possibilities, it will be important to elucidate and compare the pathways regulated by Hand2 in each of these contexts, as well as in other settings, such as the Hand2-driven induction of hypertrophy in the postnatal mouse myocardium (Dirkx et al., 2013). In the long term, these investigations may allow further improvements in strategies for cardiac reprogramming, regeneration and repair.

In addition to their implications regarding future applications for Hand2 in regenerative medicine, our results provide intriguing insight into possible causes of CHD. Duplications and deletions of the 4q33 chromosomal region, which contains *HAND2*, have been associated with CHD (Borochowitz et al., 1997; Byatt et al., 1997). Moreover, individuals with partial trisomy distal 4q (4q+ syndrome), a translocation that involves duplication of *HAND2* and neighboring genes, exhibit striking cardiac and limb defects (Tamura et al., 2013). In a mouse model for 4q+ syndrome, rebalancing levels of *Hand2* by breeding to *Hand2*-deficient animals ameliorated the heart and limb phenotypes, implicating overexpression of *Hand2* as a cause of these defects (Tamura et al., 2013). Our data suggest possible ways in which *HAND2* overexpression could cause CHD through alteration of cardiomyocyte production; future studies that elucidate the specific Hand2 partners and targets involved in FHF specification, SHF proliferation and cardiomyocyte proliferation will provide a deeper understanding of the mechanisms through which Hand2 influences the origins of CHD.

MATERIALS AND METHODS

Zebrafish and genotyping

We bred wild-type zebrafish, zebrafish heterozygous for the *hand2* mutant allele *han*^{s6} (Yelon et al., 2000) or zebrafish carrying *Tg(-5.1myl7:nDsRed2)*^{f2} (Mably et al., 2003). In addition, we bred zebrafish carrying *Tg(nkx2.5:ZsYellow)* (Zhou et al., 2011) or *Tg(kdrl:GRCFP)* (Cross et al., 2003) to zebrafish carrying the newly generated transgenes described below, and we employed adult zebrafish carrying *Tg(hand2:EGFP)*^{pd24} (Kikuchi et al., 2011a). PCR genotyping of *han*^{s6} mutant embryos was conducted as previously described (Yelon et al., 2000).

Injection of mRNA

We synthesized capped mRNA from a pCS2-*hand2* plasmid using the Ambion mMESSAGE mMACHINE kit, and we injected 160 pg *hand2* mRNA into embryos at the one- to two-cell stage. The *hand2* dimerization-deficient (*hand2 P*) and DNA binding-deficient (*hand2 EDE*) constructs were generated using the QuikChange II site-directed mutagenesis kit (Agilent Technologies).

Creation of stable transgenic lines

To generate transgenes suitable for heat-activated overexpression of *hand2*, we first amplified the *hand2*-coding sequence from the plasmids pCS2-*hand2*, pCS2-*hand2 P* and pCS2-*hand2 AA*, and cloned these amplicons into the p3xFLAG-CMV vector (Sigma) at the *Hin*dIII and *Xba*I restriction sites. Each version of *FLAG-hand2* was then introduced into the pENTR/D-TOPO vector (Invitrogen). Each final transgene was achieved through a Gateway LR reaction containing four plasmids: p5E-hsp70l (Kwan et al., 2007), pDestTol2pA2 (Kwan et al., 2007), p3E-2A-mcherry-pA (Covassin et al., 2009) and the appropriate pENTR/D-TOPO *FLAG-hand2* plasmid.

We employed standard protocols to create transgenic founders (Fisher et al., 2006). The F1 progeny of prospective founder fish were screened for mCherry fluorescence following heat shock for 1 h at 37°C, and phenotypic analysis was performed on the F1 and F2 progeny of promising founders. We compared the phenotypes generated by heat shock of four lines carrying *Tg(hsp70:hand2)*, three lines carrying *Tg(hsp70:hand2*^{AA}*)* and one line carrying *Tg(hsp70:hand2*^{P}*)*, all of which exhibited qualitatively similar levels of mCherry fluorescence. Following heat shock at 10 hpf, embryos from all of the *Tg(hsp70:hand2)* and *Tg(hsp70:hand2*^{AA}*)* lines exhibited similarly abnormal cardiac morphology at 36 hpf. In addition, expression of *Tg(hsp70:hand2)* and expression of *Tg(hsp70:hand2*^{AA}*)* were both able to rescue heart tube formation in *han*^{s6} mutant embryos, whereas expression of *Tg(hsp70:hand2*^{P}*)* did not rescue. Results shown here use three specific transgenic lines: *Tg(hsp70:FLAG-hand2-2A-mCherry)*^{sd28}, *Tg(hsp70:FLAG-hand2AA-2A-mCherry)*^{sd29} and *Tg(hsp70:FLAG-hand2P-2A-mCherry)*^{sd30}.

To generate the transgenic line *Tg(β-actin2:loxp-mCherry-STOP-loxp-hand2)*^{pd38}, 5.3 kb of genomic DNA immediately upstream of the *β-actin2* transcriptional start site was subcloned into a modified pBSK vector with a multiple cloning site flanked by I-*Sce*I restriction sites. A *loxP-mCherry-STOP-loxP-hand2* cassette was then subcloned downstream of the *β-actin2* promoter. The *mCherry*-STOP cassette serves as a marker for the transgene and also prevents read-through translation of Hand2 protein.

In situ hybridization

Whole-mount *in situ* hybridization was performed as previously described (Thomas et al., 2008) using probes for *cmlc2* (*myl7*; ZDB-GENE-991019-3), *mef2cb* (ZDB-GENE-040901-7), *islet1* (*isl1*; ZDB-GENE-980526-112), *scl* (*tal1*; ZDB-GENE-980526-501), *etsrp* (*etv2*; ZDB-GENE-050622-14), *pu.1* (*spi1b*; ZDB-GENE-980526-164), *nkx2.5* (ZDB-GENE-980526-321) and *gata4* (ZDB-GENE-980526-476). Embryonic stages were determined by counting somites prior to fixation. Area measurements were made by using the selection tool in ImageJ64 to score stained pixel area. Statistical analysis of data sets was performed using Microsoft Excel to conduct unpaired *t*-tests. We have found that *cmlc2* area measurements at 18-20 somites correlate well with counts of cell outlines in the same images (data not shown), making area measurement a reasonable strategy for comparing estimated sizes of cardiomyocyte populations.

Immunofluorescence

Whole-mount immunofluorescence was performed as previously described (Thomas et al., 2008), using the monoclonal antibodies MF20 and S46 (Developmental Studies Hybridoma Bank), a polyclonal antibody against Islet1 (GeneTex; GTX128201L) and the secondary antibodies goat anti-mouse IgG2b FITC (Southern Biotech), goat anti-mouse IgG1 TRITC (Southern Biotech) and goat anti-rabbit Alexa Fluor 488 (Molecular Probes). The numbers of Islet1-positive nuclei within MF20-positive cells were counted both in three-dimensional reconstructions and in optical sections.

Fluorescent *in situ* hybridization with immunofluorescence

Embryos were fixed in 2% formaldehyde for 20 min and then gently agitated in 0.5% Triton and 0.2% saponin to dissolve the yolk. Embryos were then fixed in 4% paraformaldehyde overnight at 4°C. An antisense *mef2cb* probe was detected by deposition of TSA Plus fluorescein solution (PerkinElmer), using an established protocol (Brend and Holley, 2009), followed by MF20 antibody staining.

Cell counting and EdU incorporation

Cardiomyocyte counting in *Tg(-5.1myl7:nDsRed2)* embryos was performed using an established protocol (Schoenebeck et al., 2007). Cell counting in *Tg(hsp70:FLAG-hand2-2A-mCherry)* embryos was performed subsequent to EdU incorporation, using a modification of a described protocol (Zeng and Yelon, 2014). Dechorionated embryos were exposed to 10 mM EdU in

Development (2014) 141, 3112-3122 doi:10.1242/dev.106336

0.3× Danieau buffer with 15% DMSO for 30 min on ice. After a series of washes, embryos were incubated at 28.5°C until fixation. Embryos were fixed in 2% formaldehyde for 20 min and then gently agitated in 0.5% Triton and 0.2% saponin to dissolve the yolk, followed by fixation in 2% formaldehyde overnight at 4°C. Embryos were then stained with the primary antibody MF20 followed by an anti-mouse IgG secondary antibody conjugated with either Alexa Fluor 488 or 647 (Invitrogen). EdU incorporation was visualized using a Click-iT imaging kit (Invitrogen) with either Alexa Fluor 594 or 647. Samples were then placed in SlowFade Gold anti-fade reagent with DAPI (Molecular Probes). Cardiomyocyte number was determined by examining DAPI-stained nuclei within MF20-positive cells both in three-dimensional reconstructions and in optical sections, and proliferation index was calculated as the percentage of these cells that exhibited EdU localization. A similar method was used to determine the number and proliferation index of *Tg(nkx2.5:ZsYellow)*-expressing MF20-negative cells clustered near the arterial pole of the heart tube. Statistical analysis of data sets was performed using Microsoft Excel to conduct unpaired *t*-tests.

Imaging

Bright-field and fluorescent images were captured with a Zeiss Axiocam on a Zeiss Axiozoom or a Zeiss Axioplan microscope, and processed using Zeiss AxioVision and Adobe Creative Suite. Confocal *z*-stacks were collected by a Leica SP5 confocal microscope and analyzed using Imaris software (Bitplane).

Cardiac injury and histology

For cardiomyocyte ablation injury, we induced myocyte expression of diphtheria toxin A in zebrafish carrying both the *Tg(cmlc2:CreER)*^{pd10} (Kikuchi et al., 2010) and *Tg(β-actin2:loxp-mCherry-STOP-loxp-DTA)*^{pd36} (Wang et al., 2011) transgenes; this combination is referred to as Z-CAT (zebrafish cardiomyocyte ablation transgenes) (Wang et al., 2011). Anesthetized Z-CAT fish were injected with 0.5 mg/ml 4-hydroxytamoxifen (4-HT) in 10% ethanol or with vehicle alone, as previously described (Kikuchi et al., 2010). For ventricular resection injury, we performed surgeries as described previously (Poss et al., 2002).

For analysis of paraformaldehyde-fixed hearts, *in situ* hybridization on 10 µm cryosections was performed as previously described (Poss et al., 2002), using probes for *hand2* (ZDB-GENE-000511-1), *tbx5* (ZDB-GENE-991124-7), *nkx2.5* (ZDB-GENE-980526-321) and *tbx20* (ZDB-GENE-000427-7). Immunofluorescence with primary antibodies that recognize myosin heavy chain (F59; Developmental Studies Hybridoma Bank) and GFP (Invitrogen) was performed as previously described (Kikuchi et al., 2011b). To determine cardiomyocyte proliferation indexes, we employed established techniques for staining sections with antibodies against Mef2 (Santa Cruz Biotechnology) and PCNA (Sigma), and assessing the proportion of Mef2-positive cells that are also PCNA positive (Wang et al., 2011).

Acknowledgements

We thank K. Birnbaum, N. Chi, S. Evans, T. Evans, H. Knaut, R. Lehmann, N. Tanese and members of the Yelon laboratory for thoughtful input.

Competing interests

The authors declare no competing financial interests.

Author contributions

Y.L.S., J.W., K.D.P. and D.Y. designed these studies; Y.L.S., K.M.G. and J.W. performed experiments; B.A.F. and A.B.F. generated reagents; Y.L.S., K.M.G., J.W., K.D.P. and D.Y. analyzed the data; and Y.L.S. and D.Y. wrote the manuscript with input from all authors.

Funding

This work was supported by grants to D.Y. from the National Institutes of Health (NIH) [R01HL069594 and R01HL108599], the American Heart Association and the March of Dimes; by a grant to K.D.P. from the NIH [R01HL081674]; and by grants to A.B.F. from the NIH [R01HL122123, R01HL120920 and R01AR061392]. Y.L.S. received support from an American Heart Association predoctoral fellowship [10PRE3510044]. Deposited in PMC for release after 12 months.

Supplementary material

Supplementary material available online at
http://dev.biologists.org/lookup/suppl/doi:10.1242/dev.106336/-/DC1

References

Borochowitz, Z., Shalev, S. A., Yehudai, I., Bar-El, H., Dar, H. and Tirosh, E. (1997). Deletion (4)(q33 –> qter): a case report and review of the literature. *J. Child Neurol.* **12**, 335-337.

Brend, T. and Holley, S. A. (2009). Zebrafish whole mount high-resolution double fluorescent in situ hybridization. *J. Vis. Exp.* **25**, 1229.

Byatt, S. A., Baker, E., Richards, R. I., Roberts, C. and Smith, A. (1997). Unbalanced t(4;11)(q32;q23) in a 34-year-old man with manifestations of distal monosomy 11q and trisomy 4q syndromes. *Am. J. Med. Genet.* **70**, 357-360.

Choi, W.-Y. and Poss, K. D. (2012). Cardiac regeneration. *Curr. Top. Dev. Biol.* **100**, 319-344.

Covassin, L. D., Siekmann, A. F., Kacergis, M. C., Laver, E., Moore, J. C., Villefranc, J. A., Weinstein, B. M. and Lawson, N. D. (2009). A genetic screen for vascular mutants in zebrafish reveals dynamic roles for Vegf/Plcg1 signaling during artery development. *Dev. Biol.* **329**, 212-226.

Cross, L. M., Cook, M. A., Lin, S., Chen, J.-N. and Rubinstein, A. L. (2003). Rapid analysis of angiogenesis drugs in a live fluorescent zebrafish assay. *Arterioscler. Thromb. Vasc. Biol.* **23**, 911-912.

de Pater, E., Clijsters, L., Marques, S. R., Lin, Y.-F., Garavito-Aguilar, Z. V., Yelon, D. and Bakkers, J. (2009). Distinct phases of cardiomyocyte differentiation regulate growth of the zebrafish heart. *Development* **136**, 1633-1641.

Dirkx, E., Gladka, M. M., Philippen, L. E., Armand, A.-S., Kinet, V., Leptidis, S., el Azzouzi, H., Salic, K., Bourajjaj, M., da Silva, G. J. J. et al. (2013). Nfat and miR-25 cooperate to reactivate the transcription factor Hand2 in heart failure. *Nat. Cell Biol.* **15**, 1282-1293.

Fahed, A. C., Gelb, B. D., Seidman, J. G. and Seidman, C. E. (2013). Genetics of congenital heart disease: the glass half empty. *Circ. Res.* **112**, 707-720.

Firulli, B. A., Howard, M. J., McDaid, J. R., McIlreavey, L., Dionne, K. M., Centonze, V. E., Cserjesi, P., Virshup, D. M. and Firulli, A. B. (2003). PKA, PKC, and the protein phosphatase 2A influence HAND factor function: a mechanism for tissue-specific transcriptional regulation. *Mol. Cell* **12**, 1225-1237.

Firulli, B. A., Krawchuk, D., Centonze, V. E., Vargesson, N., Virshup, D. M., Conway, S. J., Cserjesi, P., Laufer, E. and Firulli, A. B. (2005). Altered Twist1 and Hand2 dimerization is associated with Saethre-Chotzen syndrome and limb abnormalities. *Nat. Genet.* **37**, 373-381.

Firulli, B. A., McConville, D. P., Byers, J. S., III, Vincentz, J. W., Barnes, R. M. and Firulli, A. B. (2010). Analysis of a Hand1 hypomorphic allele reveals a critical threshold for embryonic viability. *Dev. Dyn.* **239**, 2748-2760.

Fisher, S., Grice, E. A., Vinton, R. M., Bessling, S. L., Urasaki, A., Kawakami, K. and McCallion, A. S. (2006). Evaluating the biological relevance of putative enhancers using Tol2 transposon-mediated transgenesis in zebrafish. *Nat. Protoc.* **1**, 1297-1305.

Garavito-Aguilar, Z. V., Riley, H. E. and Yelon, D. (2010). Hand2 ensures an appropriate environment for cardiac fusion by limiting Fibronectin function. *Development* **137**, 3215-3220.

Gupta, V., Gemberling, M., Karra, R., Rosenfeld, G. E., Evans, T. and Poss, K. D. (2013). An injury-responsive gata4 program shapes the zebrafish cardiac ventricle. *Curr. Biol.* **23**, 1221-1227.

Halloran, M. C., Sato-Maeda, M., Warren, J. T., Su, F., Lele, Z., Krone, P. H., Kuwada, J. Y. and Shoji, W. (2000). Laser-induced gene expression in specific cells of transgenic zebrafish. *Development* **127**, 1953-1960.

Hinits, Y., Pan, L., Walker, C., Dowd, J., Moens, C. B. and Hughes, S. M. (2012). Zebrafish Mef2ca and Mef2cb are essential for both first and second heart field cardiomyocyte differentiation. *Dev. Biol.* **369**, 199-210.

Jopling, C., Sleep, E., Raya, M., Martí, M., Raya, A. and Izpisúa Belmonte, J. C. (2010). Zebrafish heart regeneration occurs by cardiomyocyte dedifferentiation and proliferation. *Nature* **464**, 606-609.

Kikuchi, K., Holdway, J. E., Werdich, A. A., Anderson, R. M., Fang, Y., Egnaczyk, G. F., Evans, T., MacRae, C. A., Stainier, D. Y. R. and Poss, K. D. (2010). Primary contribution to zebrafish heart regeneration by gata4^{+} cardiomyocytes. *Nature* **464**, 601-605.

Kikuchi, K., Holdway, J. E., Major, R. J., Blum, N., Dahn, R. D., Begemann, G. and Poss, K. D. (2011a). Retinoic acid production by endocardium and epicardium is an injury response essential for zebrafish heart regeneration. *Dev. Cell* **20**, 397-404.

Kikuchi, K., Gupta, V., Wang, J., Holdway, J. E., Wills, A. A., Fang, Y. and Poss, K. D. (2011b). tcf21+ epicardial cells adopt non-myocardial fates during zebrafish heart development and regeneration. *Development* **138**, 2895-2902.

Kwan, K. M., Fujimoto, E., Grabher, C., Mangum, B. D., Hardy, M. E., Campbell, D. S., Parant, J. M., Yost, H. J., Kanki, J. P. and Chien, C.-B. (2007). The Tol2kit: a multisite gateway-based construction kit for Tol2 transposon transgenesis constructs. *Dev. Dyn.* **236**, 3088-3099.

Laflamme, M. A. and Murry, C. E. (2011). Heart regeneration. *Nature* **473**, 326-335.

Lazic, S. and Scott, I. C. (2011). Mef2cb regulates late myocardial cell addition from a second heart field-like population of progenitors in zebrafish. *Dev. Biol.* **354**, 123-133.
Lepilina, A., Coon, A. N., Kikuchi, K., Holdway, J. E., Roberts, R. W., Burns, C. G. and Poss, K. D. (2006). A dynamic epicardial injury response supports progenitor cell activity during zebrafish heart regeneration. *Cell* **127**, 607-619.
Li, Q., Kannan, A., DeMayo, F. J., Lydon, J. P., Cooke, P. S., Yamagishi, H., Srivastava, D., Bagchi, M. K. and Bagchi, I. C. (2011). The antiproliferative action of progesterone in uterine epithelium is mediated by Hand2. *Science* **331**, 912-916.
Liu, N., Barbosa, A. C., Chapman, S. L., Bezprozvannaya, S., Qi, X., Richardson, J. A., Yanagisawa, H. and Olson, E. N. (2009). DNA binding-dependent and -independent functions of the Hand2 transcription factor during mouse embryogenesis. *Development* **136**, 933-942.
Mably, J. D., Burns, C. G., Chen, J.-N., Fishman, M. C. and Mohideen, M.-A. P. K. (2003). heart of glass regulates the concentric growth of the heart in zebrafish. *Curr. Biol.* **13**, 2138-2147.
McFadden, D. G., McAnally, J., Richardson, J. A., Charite, J. and Olson, E. N. (2002). Misexpression of dHAND induces ectopic digits in the developing limb bud in the absence of direct DNA binding. *Development* **129**, 3077-3088.
McFadden, D. G., Barbosa, A. C., Richardson, J. A., Schneider, M. D., Srivastava, D. and Olson, E. N. (2005). The Hand1 and Hand2 transcription factors regulate expansion of the embryonic cardiac ventricles in a gene dosage-dependent manner. *Development* **132**, 189-201.
Nam, Y.-J., Song, K., Luo, X., Daniel, E., Lambeth, K., West, K., Hill, J. A., DiMaio, J. M., Baker, L. A., Bassel-Duby, R. et al. (2013). Reprogramming of human fibroblasts toward a cardiac fate. *Proc. Natl. Acad. Sci. USA* **110**, 5588-5593.
Palencia-Desai, S., Kohli, V., Kang, J., Chi, N. C., Black, B. L. and Sumanas, S. (2011). Vascular endothelial and endocardial progenitors differentiate as cardiomyocytes in the absence of Etsrp/Etv2 function. *Development* **138**, 4721-4732.
Poss, K. D., Wilson, L. G. and Keating, M. T. (2002). Heart regeneration in zebrafish. *Science* **298**, 2188-2190.
Provost, E., Rhee, J. and Leach, S. D. (2007). Viral 2A peptides allow expression of multiple proteins from a single ORF in transgenic zebrafish embryos. *Genesis* **45**, 625-629.
Raya, A., Koth, C. M., Buscher, D., Kawakami, Y., Itoh, T., Raya, R. M., Sternik, G., Tsai, H.-J., Rodriguez-Esteban, C. and Izpisua-Belmonte, J. C. (2003). Activation of Notch signaling pathway precedes heart regeneration in zebrafish. *Proc. Natl. Acad. Sci. USA* **100** Suppl. 1, 11889-11895.
Risebro, C. A., Smart, N., Dupays, L., Breckenridge, R., Mohun, T. J. and Riley, P. R. (2006). Hand1 regulates cardiomyocyte proliferation versus differentiation in the developing heart. *Development* **133**, 4595-4606.
Rychlik, J. L., Gerbasi, V. and Lewis, E. J. (2003). The interaction between dHAND and Arix at the dopamine β-hydroxylase promoter region is independent of direct dHAND binding to DNA. *J. Biol. Chem.* **278**, 49652-49660.
Schoenebeck, J. J., Keegan, B. R. and Yelon, D. (2007). Vessel and blood specification override cardiac potential in anterior mesoderm. *Dev. Cell* **13**, 254-267.
Song, K., Nam, Y.-J., Luo, X., Qi, X., Tan, W., Huang, G. N., Acharya, A., Smith, C. L., Tallquist, M. D., Neilson, E. G. et al. (2012). Heart repair by reprogramming non-myocytes with cardiac transcription factors. *Nature* **485**, 599-604.
Srivastava, D., Thomas, T., Lin, Q., Kirby, M. L., Brown, D. and Olson, E. N. (1997). Regulation of cardiac mesodermal and neural crest development by the bHLH transcription factor, dHAND. *Nat. Genet.* **16**, 154-160.
Tamura, M., Hosoya, M., Fujita, M., Iida, T., Amano, T., Maeno, A., Kataoka, T., Otsuka, T., Tanaka, S., Tomizawa, S. et al. (2013). Overdosage of Hand2 causes limb and heart defects in the human chromosomal disorder partial trisomy distal 4q. *Hum. Mol. Genet.* **22**, 2471-2481.
Thomas, N. A., Koudijs, M., van Eeden, F. J. M., Joyner, A. L. and Yelon, D. (2008). Hedgehog signaling plays a cell-autonomous role in maximizing cardiac developmental potential. *Development* **135**, 3789-3799.
Tsuchihashi, T., Maeda, J., Shin, C. H., Ivey, K. N., Black, B. L., Olson, E. N., Yamagishi, H. and Srivastava, D. (2011). Hand2 function in second heart field progenitors is essential for cardiogenesis. *Dev. Biol.* **351**, 62-69.
Wang, J., Panakova, D., Kikuchi, K., Holdway, J. E., Gemberling, M., Burris, J. S., Singh, S. P., Dickson, A. L., Lin, Y.-F., Sabeh, M. K. et al. (2011). The regenerative capacity of zebrafish reverses cardiac failure caused by genetic cardiomyocyte depletion. *Development* **138**, 3421-3430.
Xin, M., Olson, E. N. and Bassel-Duby, R. (2013). Mending broken hearts: cardiac development as a basis for adult heart regeneration and repair. *Nat. Rev. Mol. Cell Biol.* **14**, 529-541.
Xu, H., Firulli, A. B., Zhang, X. and Howard, M. J. (2003). HAND2 synergistically enhances transcription of dopamine-β-hydroxylase in the presence of Phox2a. *Dev. Biol.* **262**, 183-193.
Yelon, D., Ticho, B., Halpern, M. E., Ruvinsky, I., Ho, R. K., Silver, L. M. and Stainier, D. Y. (2000). The bHLH transcription factor hand2 plays parallel roles in zebrafish heart and pectoral fin development. *Development* **127**, 2573-2582.
Zeng, X.-X. I. and Yelon, D. (2014). Cadm4 restricts the production of cardiac outflow tract progenitor cells. *Cell Rep.* **7**, 951-960.
Zhou, Y., Cashman, T. J., Nevis, K. R., Obregon, P., Carney, S. A., Liu, Y., Gu, A., Mosimann, C., Sondalle, S., Peterson, R. E. et al. (2011). Latent TGF-β binding protein 3 identifies a second heart field in zebrafish. *Nature* **474**, 645-648.

```
Mouse   1    MSLVGGFPHHPVVHHEGYPFAAAAAAAAAAAASRCSHEENPYFHGWLIGHPEMSPPDYSM  60
             MSLVGGFPHHPV+HH+GY FAAAAAA      SRC HEE PYFHGWLI HPEMSPPDY+M
Fish    1    MSLVGGFPHHPVMHHDGYSFAAAAAA------SRC-HEEPPYFHGWLISHPEMSPPDYTM  53

Mouse   61   ALSYSPEYASGAAGLDHSHYGGVPPGAGPPGLGGPRPVKRRGTANRKERRRTQSINSAFA  120
             A SYSPEY++GA GLDHSHYGGVP         GPR VKRR TANRKERRRTQSINSAFA
Fish    54   APSYSPEYSTGAPGLDHSHYGGVPGAGA--VGMGPRTVKRRPTANRKERRRTQSINSAFA  111

Mouse   121  ELRECIPNVPADTKLSKIKTLRLATSYIAYLMDLLAKDDQNGEAEAFKAEIKKTDVKEEK  180
             ELRECIPNVPADTKLSKIKTLRLATSYIAYLMD+L KD+QNG  EAFKAE KKTD KEE+
Fish    112  ELRECIPNVPADTKLSKIKTLRLATSYIAYLMDILDKDEQNGGTEAFKAEFKKTDAKEER  171

Mouse   181  RKKELNEILKSTVSSNDKKTKGRTGWPQHVWALELKQ  217
             RKKE+N++LKS+ SSNDKKTKGRTGWPQHVWALELKQ
Fish    172  RKKEMNDVLKSSGSSNDKKTKGRTGWPQHVWALELKQ  208
```

Supplemental Figure S1. Mouse and zebrafish Hand2 protein sequences are highly conserved. Alignment of amino acid sequences of mouse Hand2 (NP_034532.3; top row) and zebrafish Hand2 (AAI65015.1; bottom row), generated through pairwise BLASTP (Altschul et al., 1997). Identical and similar amino acids are indicated in the middle row. The three arginines replaced in the DNA binding-deficient form of Hand2 (Hand2 EDE) are shown in red. The phenylalanine replaced in the dimerization-deficient form of Hand2 (Hand2 P) is shown in green. The threonine and serine replaced in the phosphorylation-deficient form of Hand2 (Hand2AA) are shown in blue.

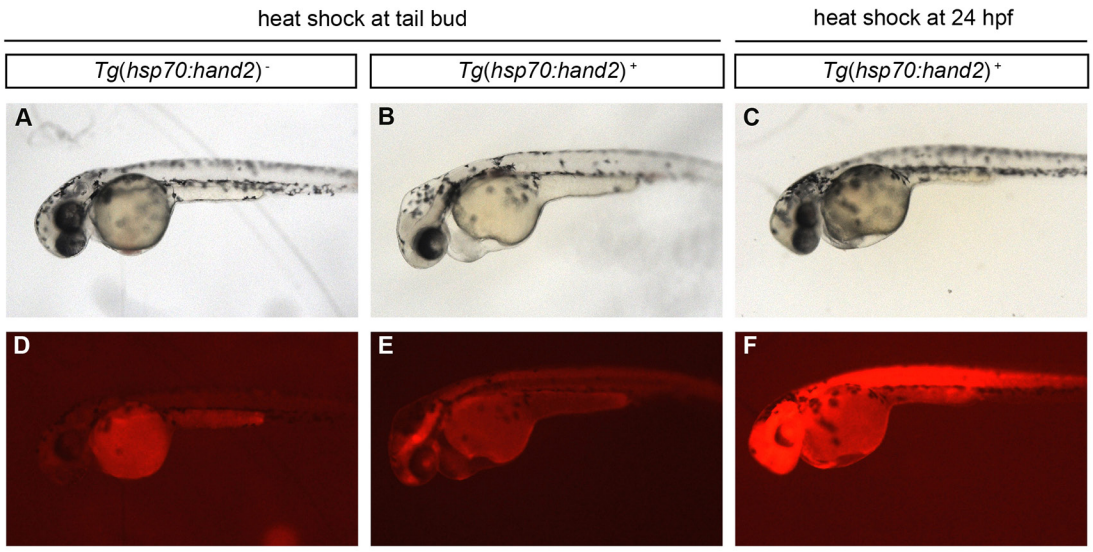

Supplemental Figure S2. Induction of *hand2* overexpression at 10 hpf, but not at 24 hpf, produces a morphologically evident cardiac phenotype. (A-F) Lateral views of live embryos at 36 hpf depict (A-C) embryonic morphology and (D-F) mCherry fluorescence in (A,D) a nontransgenic embryo and (B,C,E,F) embryos carrying the transgene *Tg(hsp70:FLAG-hand2-2A-mCherry)* (abbreviated as *Tg(hsp70:hand2)*), after heat shock at (A,B,D,E) 10 hpf (tail bud) or (C,F) 24 hpf. Heat shock of transgenic embryos at 10 hpf leads to pericardial edema (B), and residual mCherry fluorescence is still evident in these embryos at 36 hpf (E). In contrast, edema is not observed in transgenic embryos after heat shock at 24 hpf (C); mCherry fluorescence remains pervasive in these embryos at 36 hpf (F).

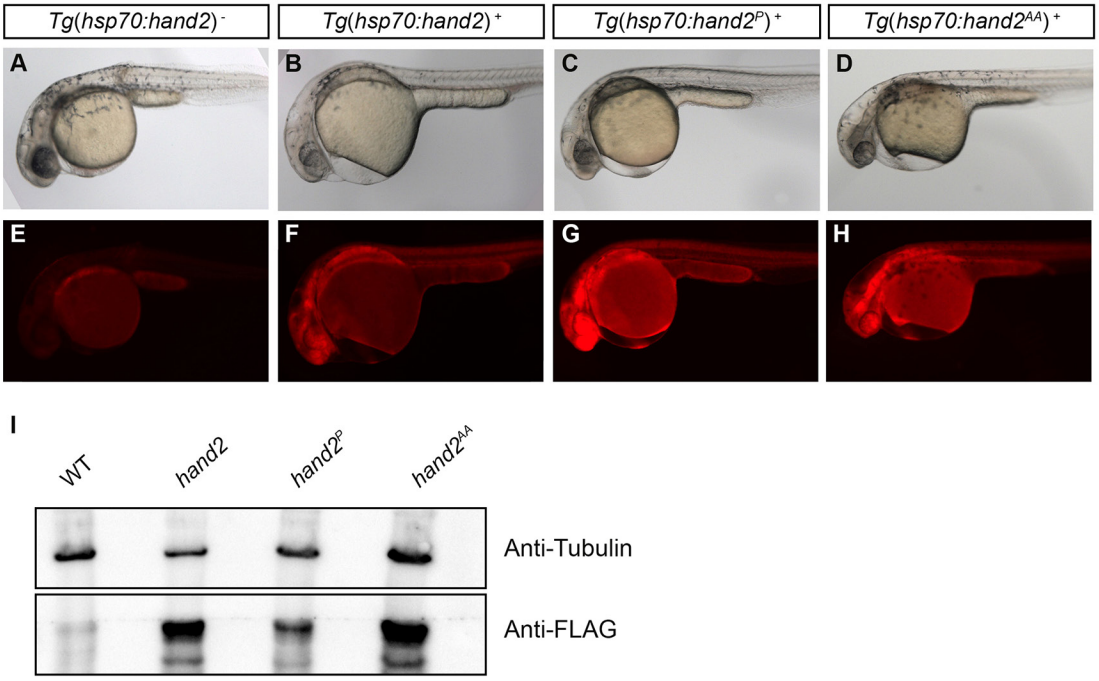

Supplemental Figure S3. Levels of protein production in different transgenic lines. (A-H) Lateral views of live embryos at 30 hpf depict bright field images of representative embryos from different transgenic lines (A-D), along with corresponding mCherry fluorescence (E-H). (E) No mCherry fluorescence is induced in heat-shocked nontransgenic embryos. (F-H) mCherry fluorescence is readily detectable in representative embryos carrying the transgenes (F) *Tg(hsp70:FLAG-hand2-2A-mCherry)* (*Tg(hsp70:hand2)*), (G) *Tg(hsp70:FLAG-hand2^{P}-2A-mCherry)* (*Tg(hsp70:hand2^{P})*), and (H) *Tg(hsp70:FLAG-hand2^{AA}-2A-mCherry)* (*Tg(hsp70:hand2^{AA})*). (**I**) Western blot analysis compares levels of FLAG-tagged Hand2 protein in different transgenic lines. Embryos were deyolked and lysates were prepared as previously described (Link et al., 2006), and blots were probed with either a monoclonal anti-FLAG M2 antibody (F1804, Sigma, 1:2000) or a monoclonal anti-α-Tubulin antibody (T6728, Sigma, 1:10,000), followed by a rabbit anti-mouse IgG HRP-conjugated secondary antibody (ab97046**,** Abcam, 1:10,000). Proteins were visualized using SuperSignal West Femto Chemiluminescent Substrate (Thermo Scientific). Each lane contains lysate from 15 embryos at 36 hpf (2 hours following heat shock), and the lanes compare protein levels in nontransgenic embryos (WT), *Tg(hsp70:hand2)* embryos *(hand2)*, *Tg(hsp70:hand2^{P})* embryos *(hand2^{P})*, and *Tg(hsp70:hand2^{AA})* embryos *(hand2^{AA})*. All three transgenic lines contain a ~23 kD FLAG-Hand2 protein, with comparable levels in *Tg(hsp70:hand2)* and *Tg(hsp70:hand2^{AA})* embryos and lower levels in *Tg(hsp70:hand2^{P})* embryos.

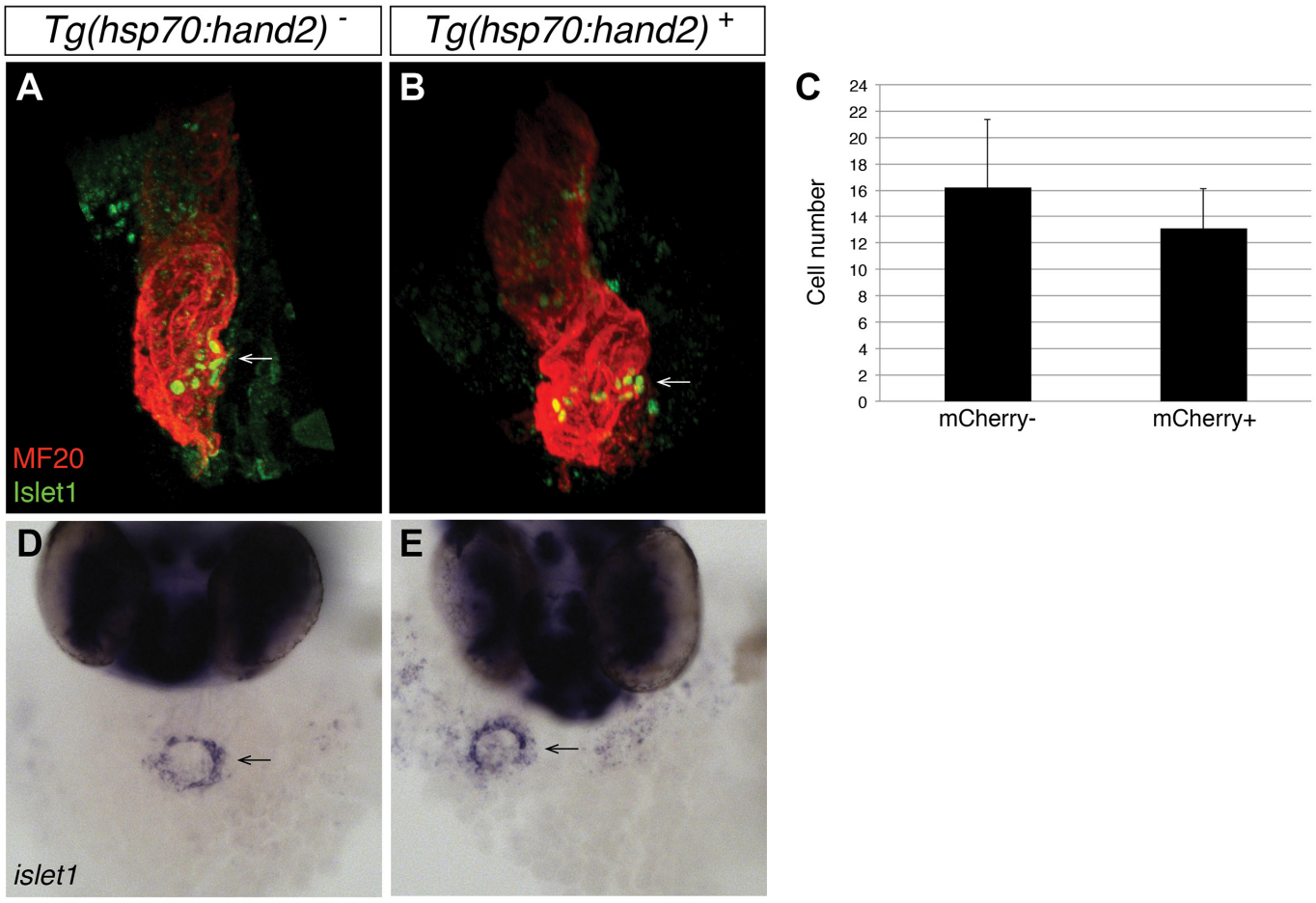

Supplemental Figure S4. Normal *islet1* expression at the venous pole in embryos overexpressing *hand2*. (A-B) Immunofluorescence at 36 hpf for MF20 (red, visible throughout the heart) and Islet1 (green, visible in the nuclei of a subset of atrial cells). Frontal views, dorsal to the top; arrows point to the Islet1-positive population at the venous pole of the atrium. Following heat shock at 10 hpf, the population of Islet1-positive cells at the venous pole appears similar in hearts from (A) nontransgenic embryos and (B) *Tg(hsp70:hand2)* embryos. **(C)** Bar graph compares average number of Islet1-positive cardiomyocytes at 36 hpf in nontransgenic embryos and *Tg(hsp70:hand2)*embryos, following heat shock at 10 hpf. Error bars indicate standard deviation; no significant difference is observed between these two data sets (n=12, p=0.09). (**D-E**) In situ hybridization depicts *islet1* expression at 36 hpf, following heat shock at 10 hpf. Frontal views, dorsal to the top; arrows point to the ring of *islet1*-expressing cells at the venous pole of the atrium. Expression patterns are similar in (D) nontransgenic embryos and (E) *Tg(hsp70:hand2)* embryos.

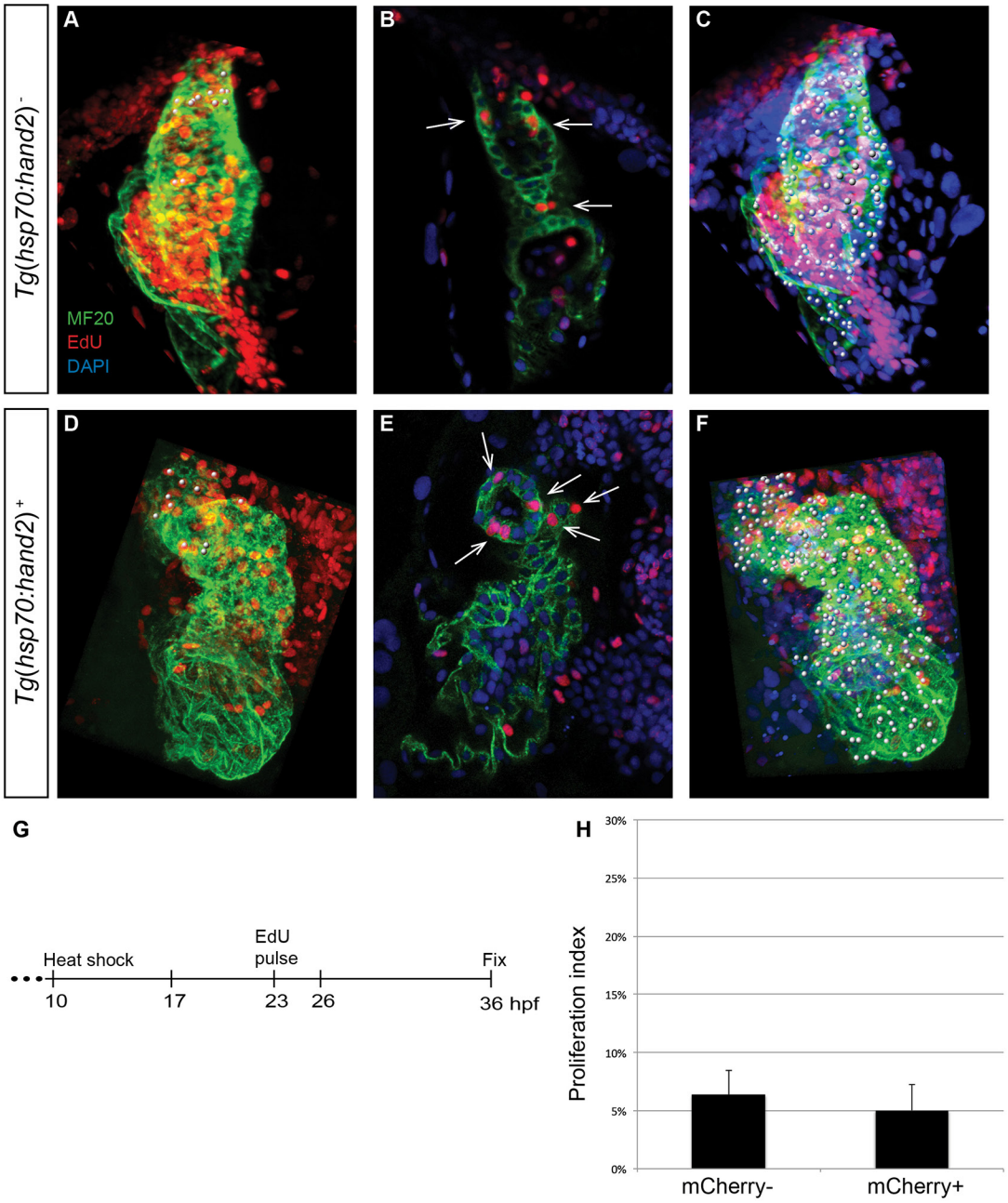

Supplemental Figure S5. No evident influence of *hand2* overexpression on cardiomyocyte proliferation after initial heart tube assembly. (A-F) EdU incorporation in hearts of (A-C) nontransgenic and (D-F) *Tg(hsp70:hand2)* embryos at 36 hpf, following heat shock at 10 hpf and EdU pulse at 23 hpf; (A,C,D,F) partial reconstructions of confocal z-stacks with ventricle up and (B,E) representative single slices. Dots, arrows, and color schemes are as described for Fig. 5A-F. Note that the nontransgenic heart shown (A) contains a number of EdU-positive blood cells that were trapped during fixation; EdU-positive blood cells are less commonly observed within the hearts of *hand2*-overexpressing embryos (D), due to their impaired circulation. **(G)** Timeline of experimental design. **(H)** Bar graph compares proliferation indexes in nontransgenic (mCherry-negative) and *Tg(hsp70:hand2)* (mCherry-positive) embryos, as in Fig. 5H. No change in proliferation index is seen in *hand2*-overexpressing embryos (n=8-11; p=0.196).

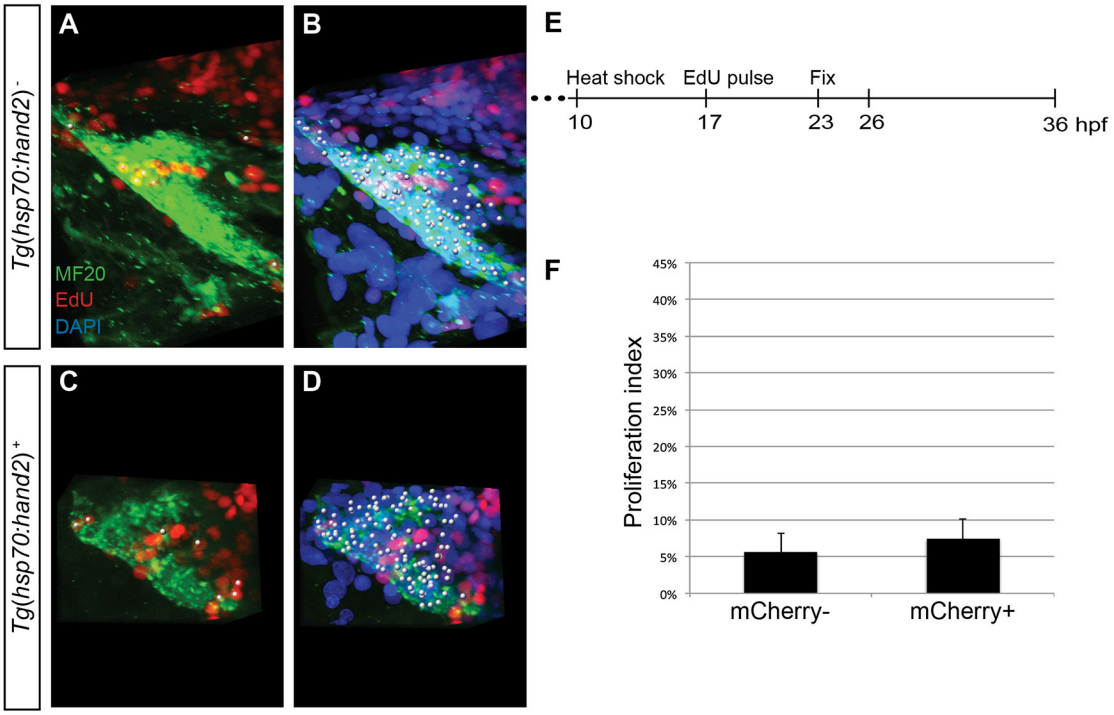

Supplemental Figure S6. No evident influence of *hand2* overexpression on cardiomyocyte proliferation within the heart tube at 23 hpf. (A-D) EdU incorporation in hearts of (A,B) nontransgenic and (C,D) *Tg(hsp70:hand2)* embryos at 23 hpf, following heat shock at 10 hpf and EdU pulse at 17 hpf; partial reconstructions of confocal z-stacks. Images depict the elongating cardiac cone, positioned with its arterial end toward the top. (A,C) White dots indicate EdU-positive (red) cells that are also MF20-positive (green) differentiated cardiomyocytes. (B,D) White dots indicate all nuclei (DAPI, blue) of myocardial cells, including both EdU-positive and EdU-negative cardiomyocytes. **(E)** Timeline of experimental design. **(F)** Bar graph compares proliferation indexes in nontransgenic (mCherry-negative) and *Tg(hsp70:hand2)* (mCherry-positive) embryos, as in Fig. 5H. No change in proliferation index is seen in *hand2*-overexpressing cardiomyocytes (n=10-11; p=0.252). Similarly, when we assessed EdU incorporation in *hand2*-overexpressing embryos at 26 hpf, following heat shock at 10 hpf and EdU pulse at 14 hpf, we did not see an increased proliferation index in *hand2*-overexpressing cardiomyocytes (proliferation index of 28 ± 4% in nontransgenic embryos compared to proliferation index of 27 ± 4% in *hand2*-overexpressing embryos; n=7-10, p=0.58).

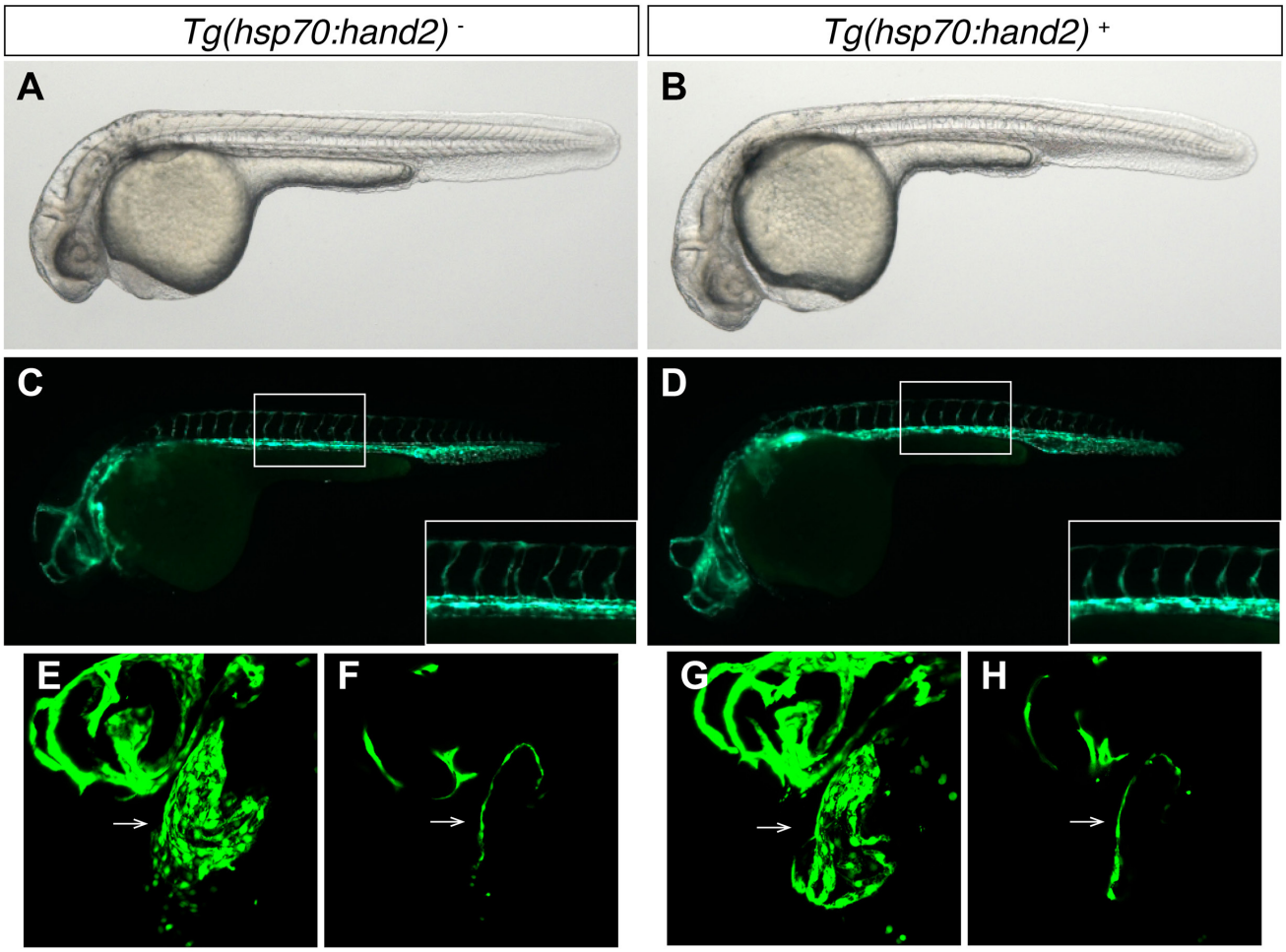

Supplemental Figure S7. Endocardium is present in embryos overexpressing *hand2*. (A-H) Lateral views of live embryos at 30 hpf depict (A-B) embryonic morphology and (C-H) expression of the transgene *Tg(kdrl:GRCFP)* in the vasculature of (A,C,E,F) nontransgenic embryos and (B,D,G,H) *Tg(hsp70:hand2)* embryos, following heat shock at 10 hpf. (C-D) General vascular patterning and sprouting of intersomitic vessels (inset) is intact in embryos overexpressing *hand2* (D). (E-H) Partial reconstructions of confocal z-stacks (E,G) and representative single slices (F,H) highlight the endocardium (arrows): just as in nontransgenic embryos (E,F), a thin layer of endocardial tissue lines the entire heart tube in embryos overexpressing *hand2* (G,H).

SUPPLEMENTAL REFERENCES

Altschul, S. F., Madden, T. L., Schaffer, A. A., Zhang, J., Zhang, Z., Miller, W. and Lipman, D. J. (1997). Gapped BLAST and PSI-BLAST: a new generation of protein database search programs. *Nucleic Acids Res* 25, 3389-3402.

Link, V., Shevchenko, A. and Heisenberg, C. P. (2006). Proteomics of early zebrafish embryos. *BMC Dev Biol* **6**, 1.